Starvation-induced autophagy via calcium-dependent TFEB dephosphorylation is suppressed by Shigyakusan

DOCTOR OF PHILOSOPHY

Center for Frontier Oral Science

Graduate School of Frontier Biosciences

Osaka University

2020 March

Sumiko Ikari

Abstract

Kampo, a system of traditional Japanese therapy utilizing mixtures of herbal medicine, is widely accepted in the Japanese medical system. Kampo originated from traditional Chinese medicine, and was gradually adopted into a Japanese style. Although its effects on a variety of diseases are appreciated, the underlying mechanisms remain mostly unclear. Using a quantitative tf-LC3 system, I conducted a high-throughput screen of 128 kinds of Kampo to evaluate the effects on autophagy. The results revealed a suppressive effect of Shigyakusan/TJ-35 on autophagic activity. TJ-35 specifically suppressed dephosphorylation of ULK1 and TFEB, among several TORC1 substrates, in response to nutrient deprivation. TFEB was dephosphorylated by calcineurin in a Ca^{2+} dependent manner. Cytosolic Ca^{2+} concentration was increased in response to nutrient starvation, and TJ-35 suppressed this increase. Thus, TJ-35 prevents the starvation-induced Ca^{2+} increase, thereby suppressing induction of autophagy.

General introduction

About autophagy

Type of autophagy

Autophagy is a major mechanism for the degradation of intracellular components in lysosomes. Three classes of autophagy, macroautophagy, microautophagy and chaperone autophagy are known in mammals because of the different mechanisms by which substrates are delivered to lysosomes.

Among these, macroautophagy has been extensively studied, and new findings on its molecular mechanisms, regulatory mechanisms, and physiological roles have been reported[1][2][3][4]. When cells are exposed to starvation or other stress, cells can obtain nutrients by degrading parts of themselves in autophagy and survive. Although each of the three autophagy pathways has its own characteristics, crosstalk between autophagy pathway has also been suggested, and there is a possibility that they are cooperation with each other.

Process of macroautophagy

Autophagy is an intracellular transport mechanism using membrane traffic. Vesicles appear in the cytoplasm and grow while curving. Finally, the tip promote scission and form an autophagosome[5]. Completed autophagosomes fuse with lysosome and the contents are degraded. The most important part of the process of autophagy is the formation of autophagy. ATG gene and Atg protein found in Atg proteins were identified as the product of 14 ATG genes essential for autophagy in *Saccharomyces cerevisiae.* All of these homologs were then identified in mammals. More than 40 Atg proteins have been identified[6][7]. Atg proteins are required for the formation of autophagosome and are conserved

in organisms including higher plants and animals. These proteins involved in the process of autophagy into four functional units[8].

1) ULK complex

When autophagy is formed by starvation, stress, etc, ULK1/2 (Atg1 in yeast) is the most upstream of Atg proteins and is the first to signal the autophagosome formation mechanism.

One is categorized the Atg1/ULK1 complex, (Atg1/ULK1, Atg13,Fip200, Atg101) for initiation formation of phagosome[6][9][10]. Atg17, Atg29 and Atg31 are also added in yeast. The homolog of Atg17, Atg31 and Atg29 has not been found in mammals. The Complex is inactivated by mTORC1 of a serine/threonine protein kinase which regulates various cellular functions including protein synthesis under nutrient rich conditions. When mTORC1 is inactivated, ULK1 and Atg13 are phosphorylated by mTORC1. mTORC1 is inactivated under starvation conditions, and the results is dephosphorylation of ULK1/2 followed by autophagosome formation.

2) PI3K complex

Autophagosome membrane contains phosphatidylinostitol3-phosphate (PI3P), and phosphoinositide 3-kinase (PI3K) to produce it is essential for autophagosome formation. Class III PI3K complex forms a complex with Beclin1 (mammalian homolog of Atg6) and Vps15 [11]. The binding of additional proteins to these proteins ultimately leads to the formation three types of complexes. Complex A contains Atg14 in addition to a common subunit. Complex B contains UVRAG instead of Atg14. Complex C contains Rubicon in addition to UVRAG. Yeast does not have Rubicon homolog Complex A is required for autophagosome formation. Complex B controls the fusion of autophagosome with lysosome. Complex C negatively regulates the fusion of autophagosome with lysosome.

3) Atg9 and VMP1

Atg9 is the only transmembrane protein among Atg proteins. There are an important role of Atg9 for phagosome expansion and its recycling system (Atg2, Atg9, and Atg18) for phagophore expansion[12][13]. VMP1 is a transmembrane protein that is homolog absent in yeast. VMP1 is located in the endoplasmic reticulum and acts late in autophagosome formation.

4) LC3 cascade

When the PI3K complex and other proteins initiate the formation of isolation membrane, LC3 (the mammalian homolog of Atg8) binds to it. LC3 is cleaved by the cysteine protease Atg4 and yield LC3-Ⅰ. Covalent rink of phosphatidylethanolamine (PE) to the c-terminus of LC3-Ⅰ in the cytoplasm results in LC3-Ⅱ, which is localized to the isolation membrane[14]. This covalent binding reaction with lipid is catalyzed by Atg7 and Atg3[15][16]. On the other hand, Atg5 binds to Atg12 via ubiquitin-like modification reaction catalyzed by Atg7 and Atg10, and then form a complex with Atg16L. This complex catalyzes the final in lipidation by binding Atg12 to Atg3 bound to LC3. At the time, Atg16L recognizes the membrane where lipidation occurs[17][18]. When the autophagosome fuses with the lysosome, the inside of the LC3 is degraded, and the outside bound LC3 is released. Therefore, the progress of autophagy can be monitored by measuring the degradation of LC3[14].

mTOR and Autophagy (upstream of autophagy)

Tor is involved in the control of autophagy in the yeast, *Saccharomyces cerevisiae*. The induction of autophagy in response to starvation in the most fundamental control of autophagy, from yeast to humans. The principal mammalian role is mTOR (mammalian target of rapamycin). mTOR is a

serine/threonine kinase found as an intracellular target of the immunosuppressant, the anticancer drug rapamycin. This is the same as yeast. mTOR functions as two different complexes (mTORC1 and mTORC2), depending on the subunit to which it binds.

When amino acids and growth factors are sensed, mTORC1 activates biosynthesis transcription, and translation of protein lipid nucleic acids through phosphorylation, and contributes to cell growth and proliferation. Activation of mTORC1 also inhibits autophagy. Among of TOR complexes, only TORC1 is inhibited by rapamycin, and TORC2 is insensitive to rapamycin.

mTORC1 activation mechanism

As in yeast, the suppression of mTORC1 activity under starvation conditions results in the induction autophagy. Insulin is involved in the regulation of mTORC1, and the cascade of class IPtdins3 kinases ～ PDK1 ～ AKT, which phosphorylates and inactivates TSC2, thereby maintaining mTORC1 activation and inhibiting autophagy. Since TSC2 is a GAP of the small G protein Rheb, which is an activator of mTORC1, its inactivation means activation of mTORC1. Amino acid are the most important regulators of mTORC1. A complex of the small G protein RagD and RagB binds to mTORC1 under nutrient rich conditions. Because the Rag complex is anchored to the lysosomal membrane by protein complex Ragulator, mTORC1 also binds the lysosome. The presence of Rheb in the lysosomal membrane results in activation of mTORC1.

mTORC2 activations mechanism

mTORC2 is responsible for phosphorylation of hydrophobic motifs involved in the activation of Akt and PKC. mTORC2 like mTORC1 is also activated by insulin. The mechanism of mTORC2 activation is not well understood, although it has been reported that ribosome binding is important for its activation. Activation of PI3 kinase by insulin activates mTORC2 by binding to ribosomes.

Function in the mTOR

mTORC1 is activated by phosphorylation of ULK1 and TFEB of mTORC1 substrates which involved in autophagy, and S6K and 4EBP1 of mTORC1 substrates which involved in cell proliferation and protein synthesis. mTORC2 is closely related to the mTORC1 signaling pathway trough phosphorylation of Akt, PKC and others. In addition, an independent of mTORC2 is the regulation of the actin skeleton.

Autophagy and disease

Recently, research on autophagy and human disease is active. For example, ATG16L1 was identified as a risk allele of inflammatory bowel disease Crohn disease in 2007[19]. It has also been reported that Atg16L1, which is involved in Crohn disease, modulates endotoxin-induced inflammasome activation in mice. This study indicates that Atg16L1 is an essential component of autophagy processes involved in the regulation of endotoxin-induced inflammatory immune responses[20]. Other than that, it was reported that autophagy degradation of mitochondria with reduced membrane potential was associated with the familial Parkinson's disease causative gene Parkin/PARK2, another associated factor in familial Parkinson's disease, and phosphorylated ubiquitin[21][22]. Thus,

Parkinson's disease caused by mutations in Parkin and PINK1 is thought to be caused by accumulation of defective mitochondria, which should have been degraded by defective mitophagy.

Other than that, it was found a mutation in the WDR45/WIPI4 gene as a cause of SENDA[23]. WIPI4 is a human homolog of yeast ATG18 or ATG21 (WIPI 1～4 in mammals). WDR 45 is a gene encoded by the X chromosome, and most patients are female mosaics. SENDA is a neurodegenerative disease characterized by iron deposition in the brain, including the basal ganglia. It show non-progresses rapidly to Parkinson disease-like symptoms after the age of 20～30 years. It was confirmed that autophagy activity is reduced in patient lymphoblasts[23].

Autophagy maintain homeostasis of not only normal cells but also cancer cells and helps them survive. Rather, cancer cells tend to require more autophagy function than normal cells because of their vigorous energy expenditure and metabolic stress in the harsh cancer microenvironment. For autophagy and cancer research, attempts to target autophagy have already begun. The drug under clinical trial is the effect of chloroquine for malignant tumors[24]. Chloroquine is a drug that inhibits lysosomal function, and although not necessarily specific for autophagy, it used as autophagy inhibitor. In 2016, 27 cases of hydroxychloroquine and 8 cases chloroquine were registered as Phase 1～2 on ClinicalTrials.gov of the NIH. It is already effective in some patients. There are various theories as to why autophagy inhibition is effective in treatment of cancer. It may result from inhibition of autophagy not only as a function of amino acid production, but also as a function of wide cellular remodeling and quality control mechanisms. If I can develop drugs that specifically inhibit autophagy, more effective cancer drugs will be developed.

About Kampo

History of traditional herbal medicine (Kampo)

Kampo is a traditional Japanese medicine that has been introduced from China and developed in japan since ancient centuries. It was originally generated in China, and over the years, the Japanese style was modified to suit the Japanese body and Japanese climate and developed uniquely. Japan has imported various cultures from China. Around the sixth century, traditional Chinese medicine (TCM) was introduced from the Korean Peninsula to Japan. Japanese envoys to Chinese Sui and Tang Dynasty came to China, and after the 7th century, various medical books were imported along with Chinese culture. Kampo was established in the Edo period. It is said that the name of “Kampo” came to be used to distinguish it from “Dutch” of a Dutch medicine imported from Nagasaki. After the Meiji period, we called traditional Japanese medicine based on Chinese medicine “Kampo” to Western medicine.

Present state of Kampo

Kampo medicine has been established based on the theory of Kampo medicine using natural materials such as plants, animals and minerals. Kampo was originally a traditional medicine developed in China. Since the listing of herbal medicines in the National Health Insurance (NHI) Drug Price List in 1967, 89% of doctors have prescribed Kampo medicines. The reason for this is that doctors have been promoting the use of Kampo[25], which is intended to treat the disorder of the while body of disease and to correct it properly, because it is useful for symptoms and diseases that are difficult to cure in Western medicine. Kampo has various forms such as decoction, powder and pill, and it thought that

the appearance of extracts made by processing the birth of Kampo to make them easy to take and the fact that they became easy to take also greatly influenced the popularization of Kampo. Generally, Kampo is composed of several kinds of crude drugs containing various bioactive substances. Although the compounds in these crude drugs are considered to be the main components of bioactivity, identification of the active ingredients and elucidation of the mechanism of action are difficult. Evidence has been accumulated, but there are few at present.

Mechanism of action of Kampo

Recently, mechanism of action and new efficacy of Kampo are reported. Yokukansan (TJ-54) was originally prescribed to treat neurosis and crying at night, but recent studied have shown that it inhibits effects on the serotonergic system and excitation of the glutamatergic system. It is used to treat dementia by suppressing BPSD such as aggressive behavior of dementia and hallucinations[26]. Rikkunshito (TJ-43) promotes the secretion of ghrelin, an appetite hormone, and is reported to be effective for anorexia[27]. Daikenchuto (TJ-100) has been reported to enhance intestinal motility by stimulation acetylcholine secretion and motilin secretion, and to be effective in the treatment of paralytic ileus after recovery surgery[28].

Introduction of This thesis

When cells experience nutrient starvation, they start to degrade themselves by a process called autophagy. During autophagy, membrane structures called autophagosomes are generated and enwrap their targets, including cytosolic proteins and organelle, and delivers them to the lysosome for degradation. The degradation products, including amino acids, are recycled to sustain cellular homeostasis. The discovery of a series of autophagy-related (Atg) proteins, which participate in the formation of an autophagosome, paved the way toward the explosive expansion of autophagy studies; these proteins provide tools for exploring autophagy, which is related to multiple physiological phenomena[29].

In particular, autophagy is closely connected to various diseases, including cancer, neurodegenerative diseases, and infections[30]. For example, autophagy plays a crucial role in promoting tumor survival and growth in progressing cancers[31]-[32]. Consistent with this, administration of an autophagy inhibitor, hydroxychloroquine, dramatically reduces tumors size[33]. However, hydroxychloroquine has severe side effects, including damage to the retina[34]. Accordingly, the development of novel, safe, and feasible autophagy-modulating drugs has attracted a great deal of attention in both academic research and the pharmacological industry[35]-[36].

Traditional herbal medicine is a potential source of autophagy modulators. In fact, multiple studies have reported the effects of herbal medicine on autophagy[37]. In Japan, there is a system of traditional therapy, Kampo, that utilizes mixtures of herbal medicines[38]. After originating in traditional Chinese medicine, it was gradually adopted into a Japanese style over the past centuries, and is now widely accepted by the Japanese medical system as over-the-counter or prescription drugs. Kampo medicines

are combinations of multiple herbs with standardized dried extract formulations. Although its effects on a variety of diseases are appreciated, the underlying mechanisms remain mostly unclear. Because it is already accepted as a prescribed drug, Kampo will be relatively easy to apply to the clinical phase as drug repositioning after another efficacy like autophagy modulator. Furthermore, Kampo medicines are generally low-cost and have limited side effects, which makes their application more attractive.

In this study, I screened 128 Kampo medicines to search for autophagy modulators. In addition to the aforementioned expectation of future clinical application, knowledge of the detailed mechanisms by which Kampo interferes with autophagy will provide insight into the regulation of autophagy. To date, very few studies have focused on the relationship between Kampo and autophagy[39]·[40]. I took advantages of our original tf-LC3 screening system, which could quantitatively estimate the effect of each drug on autophagy[41]. I identified TJ-35/Shigyakusan as a potent autophagic inhibitor, and found that it perturbs the calcium-dependent mechanism of autophagy induction.

Results

Screening of Kampo for effects on autophagy

First, I explored the effect of Kampo extracts on autophagic activity by taking advantage of tf-LC3, a trimeric chimera of GFP, RFP, and LC3, which is an autophagosomal membrane protein transported into the lysosome (Fig 1A)[42]. As autophagy progresses, GFP signal is attenuated due to its sensitivity to the acidic environment of the lysosome, whereas the RFP signal is maintained[42]. Hela cells stably expressing tf-LC3 were cultured in the presence of 128 kinds of Kampo extract, and the signal intensity of GFP and RFP in each view field was measured after 24 hours (Fig 1B, C), 48 hours (Fig 1D), and 72 hours of incubation (Fig 1E). To determine Torin-1 and Bafilomycin A concentration, I followed standard treatment conditions described previously[42][43]. For determining Kampo concentration, I pre-screened small scale samples (20 samples) with different concentrations (100, 200, 400 μg/ml), and the concentration of 400 μg/ml exerted the most prominent effects; accordingly, I adopted it. In comparison to vehicle control, some Kampo treatments decreased the GFP/RFP signal ratio at each time point, as did the known autophagy inducer, Torin-1[43]. These represent candidates for autophagy inducers that could be examined in future studies. On the other hand, three kinds of Kampo, TJ-35, TJ-122, and TJ-133, increased the GFP/RFP signal ratio at each time point, similar to the known autophagy inhibitor bafilomycin A_1 [44].

To further narrow down the candidates, I cultured HeLa cells expressing tf-LC3 under starvation conditions for 6 hours in the presence of these Kampo. TJ-35 treatment significantly decreased the number of GFP- and RFP-positive puncta in starvation medium. These results suggest that TJ-35 affects starvation-induced autophagy. To explore the effect of TJ-35 on other types of

autophagy, I investigated the effect on aggrephagy, which targets aggregated proteins[45]. When the cells were treated with puromycin, numerous protein aggregates were formed that were colocalized with p62, which is an adaptor protein recruited to protein aggregates (Fig 2)[46]. After puromycin was washed out, autophagy efficiently cleared protein aggregates (Fig 2). The presence of TJ 35 did not affect aggrephagy, suggesting the specific effect of TJ-35 on starvation-induced autophagy.

TJ-35 suppresses autophagosome formation under starvation condition

When tf-LC3–expressing HeLa cells were shifted from nutrient-rich medium (DMEM) to starvation medium (EBSS), the number of GFP puncta increased, primarily representing autophagosomes and forming autophagosomes, i.e., isolation membranes/phagophores (Fig 3A)[41]. However, TJ-35 treatment decreased the number of GFP-LC3 and RFP-LC3 puncta (Fig 3A). I also observed endogenous LC3 by immunofluorescence, and again the number of LC3-positive puncta was decreased by TJ-35 treatment (Fig 3B). LC3 is covalently conjugated to phosphatidyl ethanolamine to yield the LC3-II form, which is eventually degraded in the lysosome; treatment with the lysosomal activity inhibitor bafilomycin A_1 treatment inhibits this degradation, causing LC3-II to accumulate (Fig 3C, D) [47]. Although LC3-I band was scarcely detected, the bands that appeared were confirmed to be LC3-II by comparing them with those of the MEF cell samples (Fig 3E). However, TJ-35 treatment suppressed this LC3-II accumulation (Fig 2C). Together, these results established that TJ-35 treatment suppressed autophagy progression.

TJ-35, Shigyakusan, is composed of four types of crude drug, namely, bupleurum root, peony root, immature orange, and Glycyrrhiza. To assess the role of each ingredient, I omitted each

ingredient while preparing TJ-35. Omission of any of the four crude drugs resulted in failure of autophagy suppression, indicating that the combination of these ingredients is critical (Fig 4).

I next sought to determine whether TJ-35 affects autophagosome formation. Atg5 is a protein associated with forming autophagosomes (i.e., isolation membranes/phagophores), and is detached from the membrane after completion of autophagosome formation[48]. Therefore GFP-Atg5–positive structures represent isolation membranes/phagophores. When HeLa cells expressing GFP-Atg5 were incubated in starvation medium, EBSS, GFP-Atg5–positive punctuate structures were observed, indicating that autophagosome formation was proceeding (Fig 5A). However, when TJ-35 was present in the medium, the number of GFP-Atg5–positive punctate structures were significantly reduced (Fig 5A). Ulk1 is a protein kinase that forms a protein complex with FIP200/RB1CC1, ATG101, and ATG13, and makes scaffolds when autophagosome formation is induced[49]. Hela cells expressing ULK1-EGFP contained punctate signals under starvation, but these signals were much less abundant following TJ-35 treatment (Fig 5B). WIPI1 is recruited to the isolation membranes/phagophores and autophagosome via its ability to bind phosphatidylinositol 3-phosphate[50]. The number of GFP-WIPI1–positive punctate structures under starvation was also decreased by TJ-35 treatment (Fig 5C).

I also observed endogenous LC3 in the presence of Bafilomycin A1 by immunofluorescence. When the nutrient rich medium was changed to starvation medium in the presence of Bafilomycin A_1, LC3-positive puncta accumulated. However, when TJ-35 was present in the medium, the number of LC3-positive punctate structures was significantly reduced despite the present of Bafilomycin A_1 (Fig 6).

Collectively, these data indicated that TJ-35 treatment suppresses autophagy at the step before autophagosome formation.

TJ-35 suppresses dephosphorylation of ULK1 and TFEB specifically among mTORC1 substrates

I therefore asked whether TJ-35 treatment affects mTORC1 activity, a protein kinase that pivotally regulates autophagy upstream of Atg proteins[51]. TFEB is a transcriptional factor, whose localization is under the control of mTORC1 activity. Under nutrient-rich conditions, mTORC1 is active, and TFEB is phosphorylated and retained in the cytoplasm, whereas under starvation, dephosphorylated TFEB translocates to the nucleus[52]. However, when cells were treated with TJ-35, TFEB was still mostly localized in the cytoplasm even though the cells were experiencing starvation (Fig 7A). Upon entering the nucleus, TFEB up-regulates transcription of lysosome- and autophagy-related genes, including ATPV6 and LAMP1[52](Fig 7B). However, TJ-35 treatment suppressed that up-regulation (Fig 7B). These data raised the possibility that inactivation of mTORC1 during starvation is abrogated by TJ-35 treatment.

To further test this hypothesis, I examined other substrates of mTORC1. To this end, HeLa cells were cultured under starvation conditions with or without TJ-35 and subjected to western blot. Multiple sites on ULK1 protein kinase involved in autophagy, including serine-757, are dephosphorylated upon starvation and mTORC1 inhibition[53]. TJ-35 treatment suppressed this dephosphorylation (Fig 7C). The band size of TFEB was shifted down in response to starvation, indicative of dephosphorylation (Fig7D). However, the downshift was significantly suppressed in the

presence of TJ-35, consistent with the above result (Fig 7D). Unexpectedly, however, the other major mTORC1 substrates, ribosomal protein S6 kinase (S6K) were dephosphorylated normally even in the presence of TJ-35 (Fig 7E)[54]. As for another substrate of mTORC1, western blotting with anti-translation initiation factor 4E-binding protein (4EBP1) antibody reacted with both phosphorylated and unphosphorylated 4EBP1, with the latter represented by the down-shift of the band size. Dephosphorylation of 4EBP1 was also unaffected by TJ-35 (Fig 7E). Collectively, these findings indicate that TJ-35 affects dephosphorylation of only some mTORC1 substrates, namely ULK1 and TFEB, which play pivotal roles in autophagy regulation.

TJ-35 specifically suppresses dissociation of ULK1 and TFEB from mTOR under starvation conditions

To substantiate the above results, I examined the physical association among mTORC1 and its substrates by the proximity ligation assay (PLA). In this experimental system, spe cific antibodies against two different antigens give rise to punctate fluorescent signals if the antigens are within 40-nm proximity[55]. HeLa cells stably expressing ULK1-EGFP cultured under nutrient-rich conditions were subjected to PLA using antibodies against GFP and the mTOR; 4.0 ± 1.1 fluorescent signals were detected per cell (Fig 8A). These signals represented mTOR-ULK1 proximal associations, as omitting either antibody abolished the signals (Fig 8D). These signals were less abundant (1.3 ± 1.1 per cell) under starvation conditions (Fig 8A). These support previous co-immunoprecipitation data showing that mTORC1 is associated with ULK1 under nutrient-rich conditions, and dissociates after starvation[56]. However, when cells were cultured with TJ-35, the reduction in the fluorescence

signals under starvation conditions was suppressed, indicating that TJ-35 prevented the proteins from dissociating (Fig 8A). An interaction between TFEB and mTOR has also been reported[57]. HeLa cells stably expressing GFP-TFEB were subjected to PLA with anti-GFP and anti-mTOR antibodies. As with ULK1, I observed a nutrient-dependent association TFEB with mTOR, and TJ-35 treatment suppressed dissociation during starvation (Fig 8B). By contrast, although I also observed a nutrient-dependent association between mTOR and FLAG-S6K, I did not see any TJ-35–dependent suppression of dissociation during starvation (Fig 8C)[58]. These results indicate that TJ-35 affect the dissociation between mTOR with ULK1/TFEB, but not with S6K, supporting the idea of a dephosphorylation defect specific to the former two substrates.

TJ-35 suppresses cytosolic Ca^{2+} increment under starvation conditions

TFEB dephosphorylation and nuclear translocation are suppressed by knockdown of the catalytic subunit (PPP3CB) of the calcineurin, a protein phosphatase activated by Ca^{2+}[59]. I confirmed this point via a different assay. When cells were incubated with the calcium ionophore ionomycin (final, 3 μM), causing an influx of calcium from the medium into the cells, TFEB was dephosphorylated (Fig 9). However, this dephosphorylation was inhibited by treatment with cyclosporin A, an inhibitor of calcineurin[60], in a dose-dependent manner (Fig 9). Similar results were obtained with NFAT, a well-established calcineurin substrate (Fig 9)[61], supporting the idea that TFEB is a bona fide substrate of calcineurin. ULK1, S6K, and 4E-BP were not dephosphorylated by ionomycin treatment (data not shown).

Accordingly, I investigated whether the cytosolic calcium concentration is affected by starvation. For this purpose, HeLa cells were stained with the fluorescent Ca^{2+} chemical probe Fluo-8[62]. Fluorescent signals increased under starvation conditions relative to nutrient-rich conditions (Fig 10A). Based on values from the positive control (ionomycin-treated cells) and negative control (BAPTA treatment), I calculated that the calcium concentration was about 196 nM under nutrient-rich conditions and 618 nM under starvation conditions (Fig 10A). To rule out the possibility that this is due to some artifact of Fluo-8, I employed another calcium probe, G-CaMP3, a GFP-based proteinaceous probe[63]. A similar increment was observed after the shift to starvation (353 nM) from nutrient-rich medium (88 nM) (Fig 10A). These results highlighted the novel observation that starvation conditions increase the cytosolic calcium concentration.

I also treated the cells with ionomycin and cyclosporin A to see if any effects could be observed on autophagy. It has been reported that ionomycin treatment for 24 h results in massive accumulation of autophagosomes[64]. I treated the cells for 30 min, and consequently, ionomycin treatment in DMEM led to an accumulation of GFP-LC3, supporting Ca dependent autophagy induction mechanism (Fig 11). In addition, cyclosporin A treatment in EBSS reduced GFP-LC3 formation, supporting the positive role of Calcineurin in autophagy induction (Fig 11).

I then examined the effect of TJ-35, and found that the starvation-induced increment in cytosolic [Ca^{2+}] was significantly suppressed by TJ-35 treatment in both the Fluo-8 (Fig 10B) and G-CaMP3 assays (Fig 10C). Thus, the autophagy- suppressive effect of TJ-35 could be attributed, at least in part, to this phenomenon.

To identify the source of the starvation-induced calcium influx, I investigated two possible major calcium sources: the extracellular medium and the endoplasmic reticulum[65]. Even when calcium in the medium was chelated with EDTA, starvation-induced calcium influx was normal, ruling out the possibility that the medium was the source (Fig 12A). Xestospongin C is an inhibitor of the IP3 receptor, which is a major calcium release channel in the ER[66]. When cells were treated with xestospongin C, starvation-induced calcium influx was severely defective in both the Fulo-8 and G-CaMP3 assays (Fig 12B). Collectively, these observations indicate that TJ-35 prevents starvation-induced calcium efflux from the ER mediated by the IP3 receptor.

Discussion

In this study, I comprehensively screened Kampo medicines for effects on autophagy, and elucidated an inhibitory effect of Shigyakusan/TJ-35 on autophagy. Shigyakusan/TJ-35 is composed of dried extract of Bupleurum root, Peony root, Immature Orange, and Glycyrrhiza. TJ-35 is prescribed for various inflammatory diseases such as cholecystitis, pancreatitis and gastritis[67],[68]. The mechanism of action of TJ-35 appears to involve increased gastric mucosal levels of lipid peroxide[67]; prevention of the progress of gastric mucosal lesions[68] , and scavenging of O_2 generated by the hypoxanthine–xanthine oxidase system[67]. Although definitive correlation of these diseases with autophagy are still to be determined, it is known that acute pancreatitis is relieved by suppression of autophagy[69]. Suppression of autophagy by TJ-35 is anticipated to provide insight into the overall effect of this medicine. TJ-35 showed a significant inhibitory effect of autophagy under starvation conditions even in a short time treatment (Fig 3A, B and C). Therefor I examined whether the inhibitory effect of TJ-35 was also effective for selective autophagy and found that it had no effect on aggrephagy (Fig 2). In addition, I need to examine at selective autophagy in detail.

Interestingly, the present study suggested that the combinations of components is important for the autophagy inhibitory effect of TJ-35, which is composed of four of crude drugs (Fig 4). The treatment principle of Kampo is to make up for the shortcomings and remove the excess, and the body is naturally balanced. Combination of two or more crude drugs enhances the efficacy and reduces side effects. In the other words, I obtained data suggesting that Kampo composed of crude drugs mixed in a certain ratio show high activity (Fig 4).

I found that TJ-35 suppresses dephosphorylation of two mTORC1 substrates, TFEB and ULK1, both of which are critical for autophagy induction[70],[71]. Therefore, the suppressive effect of TJ-35 on autophagy could be reasonably attributed to this finding. The point of action cannot be assigned to general mTORC1 regulation, as dephosphorylation of two other mTORC1 substrates, S6K and 4E-BP, was not affected by TJ-35 (Fig 7C,D and E)(Figure 8A, B and C). Although the mechanism regarding ULK1 remains to be determined, I succeeded in narrowing down in the TFEB-related mechanism. TFEB is a bona fide substrate of calcineurin (Fig 9)[59]. Calcium plays both pro-autophagy and anti-autophagy roles in a context-dependent manner, according to the triggering stimulus[72]. I revealed that the cytosolic calcium concentration is elevated upon shift to EBSS, and that elevation is suppressed by TJ-35 treatment (Fig 10 B and C). Because this elevation flows from the ER, mediated by IP3 receptor, TJ-35 is likely to affect the IP3 receptor and/or its upstream regulator, including the IP3. Previous work showed that calcium pooled in the lysosome is extruded in response to starvation, which activates calcineurin[59]. That study proposed that the calcium concentration is elevated locally, in the vicinity of the lysosome. Although this model could be still viable, our results showed that the calcium concentration is elevated throughout the cytoplasm under starvation (Fig 10)(Fig 13). Decuypere et al. reported that starvation treatment sensitizes the IP3 receptor when stimulated by several reagents, including ionomycin, tapshigargin, and ATP, supporting the idea that the IP3 receptor plays key roles in calcium elevation under starvation[73]. Further, they also showed that chelation of intracellular calcium by BAPTA-AM or inhibition of the IP3 receptor by xestospongin C suppressed autophagy under starvation[73]. These observations are in line with our results, and are consistent with a crucial role for calcium in starvation-induced autophagy. Thus, our results also

suggest that calcium elevation is a key regulatory step in autophagy induction, and that TJ-35 is useful for pursuing this point in relation to regulation of autophagy (Fig 13). I think I need to investigate more closely about the effect of TJ-35 on ULK1. Further studies of the detailed mechanism and *in vivo* experiments should be performed in order explore the path to clinical application of TJ-35/Shigyakusan as an anti-autophagy modulator in diverse diseases, including cancer.

Because it was a complex of crude drugs, it is very difficult to understand the mechanism of action od Kampo. However, in order to clarify the characteristics of Kampo, I continue my research to find out the possibility that Kampo work in many pathways of cells. By continuing the basic research on Kampo form the viewpoint of life science, I hope that Kampo will be more active in many medical fields.

Materials and methods

Cell culture

All cell lines were cultured with Dulbecco's modified Eagle's medium (DMEM) high glucose (D6429, Sigma-Aldrich) supplemented with heat-inactivated 10% FBS (F7524, Sigma-Aldrich) in 5% CO_2 at 37 °C. For starvation treatment, cells were gently washed twice with phosphate-buffered saline (PBS) and cultured in Earle's Balanced Salts solution (EBSS) (E3024, Sigma-Aldrich) for the indicated times. For the experiments regarding calcium influx from the medium, Hank's Balanced Salt Solution without calcium (HBSS, 14175-095 Gibco) and 20 mM HEPES buffer (1 mol/l-HEPES Buffer Solution pH 7.1~7.5 17557-94 Nacalai Tesque) was used. For LC3 flux assays, 125 nM of bafilomycin A_1 (023-11641, Wako) was added. For performing the aggrephagy experiment, 5 μg/mL puromycin was used (160-23151, Wako). For inhibiting calcineurin, 20 μM cyclosporin (TCI C2408) was used. HeLa cells stably expressing ULK1-EGFP [74], GFP-Atg5, GFP-WIPI1, tf-LC3 [41] or GFP-TFEB [75], described previously, were constructed using pMRX retroviral vector [76]. HeLa cells were obtained from Yoshimori Lab stock[77]. For retrovirus preparation, plasmids were transiently transfected into Plat-E cells using Lipofectamine 2000 (52887, Invitrogen). Related plasmids were transiently co-transfected with envelope vector pVSV-G [78]. After 36 hours, the retrovirus was harvested for infection. Stable transfection was established by retroviral infection using polybrene and selection in 2 μg/mL puromycin (160-23151, Wako).

Kampo extract preparation and screening

Kampo medicines were obtained from Tsumura, Tokyo, Japan. Ingredients of each Kampo are available at STORK (Standards of Reporting Kampo products) (http://mpdb.nibiohn.go.jp/stork/) maintained by the National Institute of Health Sciences (NIHS) of Japan. Each Kampo extract was soaked in water at 40 mg/mL in a 1.5 mL tube, and incubated at 98°C for 5 min. Debris was sedimented by centrifugation at 20,400 *g* for 10 min, and supernatants were aliquoted and stored at -20°C and used for further analysis.

For the analysis of TJ-35 (Shigyakusan) ingredients, 5.0g of Bupleurum root (004217010 Tochimoto Tenkaido), 4.0 g of Peony root (005316008 Tochimoto Tenkaido), 2.0 g of Immature Orange (002419002 Tochimoto Tenkaido), and 1.5 g of Glycyrrhiza (002018007 Tochimoto Tenkaido) were either boiled together or in one of the several combinations with omitting one ingredient in 500 mL of water, until it decreased to 250 mL. The supernatants were vaporized using a vacuum lyophilizer (LABCONCO) to produce extract powders.

Ninety-six-well glass-bottom plates (655891, Greiner Bio-One) were coated with 0.1 mg/mL collagen (Cell matrix Type I-C, Nitta Gelatin). HeLa-Kyoto cells stably expressing tf-LC3, seeded at 3,000 cells/well, were cultured with 100 μL of DMEM supplemented with 10% FBS in 5% CO_2 at 37°C for 24 hours. One microliter of each Kampo extract (final, 400 μg/mL) was added to the medium, and incubated for the indicated period. Torin-1 (final, 250 nM) was used as a control for autophagy induction. Bafilomycin A_1 (final, 125 nM) was used as a control for inhibition of autophagy. Cells were washed with PBS and fixed with 4% paraformaldehyde at room temperature for 20 min, and washed again with PBS. The samples were imaged using a CQ1 confocal quantitative image cytometer

(Yokogawa). The intensity GFP or RFP signals in each view field was measured using the CQ1 Measurement software (Yokogawa).

Antibodies

The following antibodies were used for immunoblotting and immunostaining: rabbit anti-LC3 (PM036, MBL) 1/1000(IB) 1/500(IS); rabbit anti-phospho-ULK1 (Ser757) (6888S, Cell Signaling) 1/1000: rabbit anti-TFEB (4240S, Cell Signaling) 1/2000; rabbit anti-mTOR(7C10) (2983S, Cell Signaling) 1/400; mouse anti-p70S6 kinase (49D7) (2708S, Cell Signaling) 1/1000; rabbit anti-4E-BP1 (9452S, Cell Signaling) 1/1000; mouse anti-tubulin (T9026, Sigma-Aldrich) 1/10000; mouse anti-GFP (11814460001, Roche) 1/500; rabbit anti-p62 (SQSTM1) (PM045 MBL) 1/1000; HRP-conjugated anti-rabbit secondary antibody (7074S, Cell, Signaling) 1/10000; HRP-conjugated anti-mouse secondary antibody (1031-05, Southern Biotech) 1/10000.

Western blotting

Western blotting was conducted basically as reported[15]. Cells cultured in 6-well plates were washed twice with 2 mL iced-cold PBS, lysed by adding 100–200 μL of ice-cold lysis buffer [50 mM Tris-HCl (pH7.5) 150 mM NaCl, 1% Triton X-100] containing complete protease inhibitor cocktail (11873580001, Roche) and placed on ice for 20 min. Cell extracts were sedimented by centrifugation at 20,400 *g* for 10 min at 4°C. Protein concentration of supernatants was measured using the Protein Assay Bicinchoninate kit (06385-00, Sigma-Aldrich). Supernatants were mixed with 100–200 μL of sample buffer (2% SDS, 100 mM DTT, 50 mM Tris-HCl [pH 6.8], 5% glycerol, 0.001% bromophenol

blue), incubated at 98°C for 5 min, and separated by SDS-PAGE. LC3 protein was detected using 15% polyacrylamide SDS-PAGE gels, which were made using the following regents: H_2O 1.4 mL, 1.5 M Tris-HCl (pH 8.8) 1.5 mL, 30% acrylamide/bis-acrylamide 3 mL, 10% SDS 60 μL, 10% ammonium peroxydisulfate: (APS) 50 μL, tetramethyl ethylenediamine: (TEMED) 5 μL. Stacking gel was prepared using the following reagents: H_2O 1.8 mL, 0.5 M Tris-HCl (pH 6.8) 750 μL, 30% acrylamide/bis-acrylamide 375 μL, 10% SDS 30 μL, 10% APS 30 μL, TEMED 5 μL). TFEB, S6K and 4EBP1 proteins detected using 10% polyacrylamide SDS-PAGE gels, which were made using the following reagents: H_2O 2.4 mL, 1.5 M Tris-HCl (pH 8.8), 1.5 mL, 30% acrylamide/bis-acrylamide 2 mL, 10% SDS 60 μL, 10% APS 50 μL, TEMED 5 μL. ULK1 protein detected using 7.5% polyacrylamide SDS-PAGE gels, which were made using the following regents: H_2O 2.9 mL, 1.5 M Tris-HCl (pH 8.8) 1.5 mL, 30% acrylamide/bis-acrylamide 1.5 mL, 10% SDS 60 μL, 10% APS 50 μL, TEMED 5 μL. The separated proteins were transferred to PVDF membranes (LC3: Immobilon-P, Merck Millipore; ULK1, TFEB, S6K, and 4EBP1: Hybond-P, Amersham) using transfer buffer (24 mM Tris base, 190 mM glycine, 20% methanol) by the wet transfer system (NA-1510B S/N 15J01, EIDO) at 150 mA for 1 hour. The membranes were blocked for 1 hour at room temperature in 1.0% skim milk in TBS-T (25 mM Tris base, 137 mM NaCl, 2.7 mM KCl, 0.16% HCl, 0.08% Tween 20, pH adjusted to 7.4). For phosphorylated proteins, 2.5% bovine serum albumin (A7906-50G, Sigma-Aldrich) in TBS-T was used as the blocking buffer. After blocking, the membrane was incubated for 1 hour with each primary antibody in blocking buffer at room temperature. The membrane was washed three times with TBS-T for 10 min and incubated at room temperature for 40 min with HRP-conjugated secondary antibody in blocking buffer, and then washed three times with TBS-T for 10

min. The membrane was incubated in the ECL Select western blotting detection reagent (GE Healthcare) for 5 min at room temperature. Signals were detected on a Gene Gnome-5 chemiluminescence detector (Syngene).

Microscopy

For immunofluorescence, coverslips (12-mm round, No 1S thickness, Matsunami Glass) were placed into 24-well plates (142475, NUNC), coated with 0.1 mg/mL collagen (Cell matrix Type I-C, Nitta Gelatin) for 1 hour at room temperature, and washed with PBS. Cells were seeded on the coverslips and grown to 60–80% confluence. After incubation, the cells were washed with PBS at room temperature, fixed with 4% Paraformaldehyde Phosphate Buffer Solution (163-20145, FUJIFILM) for 20 min, and washed with PBS. Samples were permeabilized by incubation with 50 μg/mL digitonin (300410, Calbiochem) in 0.2% gelatin-PBS for 10 min, and washed twice with 0.2% gelatin-PBS. Samples were blocked with 0.2% gelatin-PBS for 30 min at room temperature and incubated with primary antibodies diluted in 0.2% gelatin-PBS for 1 hour at room temperature. After three washes using 0.2% gelatin-PBS, cells were incubated with secondary antibody diluted in 0.2% gelatin-PBS (Invitrogen), and washed three times with 0.2% gelatin-PBS. Samples were mounted on glass slides in 5 μL of mounting medium [3.8mM Mowiol 4-888 (81381 ALDRICH), 3.3 M non-fluorescent glycerol (075-04751 Wako), 0.2 M Tris-HCl pH 8.5, 2.5% 1.4-diazabicyclo[2.2.2]octane (D27802 Sigma-Aldrich)]. For observation of fluorescent proteins, cells were washed with PBS once and fixed with 4% paraformaldehyde for 20 min at room temperature. The samples were washed with PBS twice, and mounted with mounting reagent. Microscopic images were acquired using a TCS SP8 (Leica,

Wetzlar, Germany) confocal laser-scanning fluorescence microscope equipped with an objective lens (HC PL APO 63x/1.40 OIL CS2, Leica). Fluorescent puncta were counted using ImageJ. For analysis of GFP-TFEB, cells positive for fluorescence in the cytoplasmic and nuclear region were counted using ImageJ.

Proximity Ligation Assay

Proximity ligation assay (PLA) was conducted using Duolink in situ-Fluorescence (Sigma-Aldrich) basically as reported[15]. HeLa cells stably expressing ULK1-EGFP[74] , GFP-TFEB[75] or transiently transfected with FLAG-S6K[75] were seeded on coverslips in 24-well plates. After culture to 60%–80% confluence on coverslips, the cells were subjected to starvation with or without TJ-35, fixed with 4% paraformaldehyde for 20 min, permeabilized with 50 μg/mL digitonin in 0.2% gelatin-PBS for 10 min, and then blocked with 0.2% gelatin in PBS for 30 min. Samples were incubated with primary antibodies including rabbit anti-mTOR (1:400), mouse anti-GFP (1:500), and an mouse anti-FLAG (1:400) diluted in 0.2% gelatin-PBS for 1 hour, and washed twice with PBS. Samples were incubated with PLA probes (anti-rabbit PLUS and anti-mouse MINUS) diluted in 0.2% gelation-PBS at 37°C for 1 hour, washed twice for 5 min with PLA wash buffer A, and incubated with PLA Ligation-Ligase solution at 37°C for 30 min. Samples were washed twice with PLA wash buffer A for 2 min, incubated with PLA Amplification–Polymerase solution for 100 min at 37°C, washed twice with PLA wash buffer B for 10 min, and washed with 0.01x wash buffer B for 1 min. Samples were mounted in Duolink II mounting medium containing DAPI (4’,6-diamidino-2-phenylindole). Fluorescent puncta were counted using ImageJ.

RT qPCR

Total RNA was extracted using TRIzol (BIO-38032, BIOLINE), and with treated with deoxyribonuclease (18068-015 Invitrogen). Reverse transcription was conducted using iScript^{TM} Adv cDNA Kit for RT-qPCR (1725038 Bio-Rad). Primer sequences for ATPV6 LAMP1[79] were described previously, and for GAPDH were (forward) aatcccatcaccatcttcca and (reverse) tggactccacgacgtactca. Relative expression levels were monitored using an Applied Biosystems StepOnePlus^{TM} with the Ct method.

[Ca2+] measurement

For the Fluo-8 method, HeLa cells were seeded on glass-bottom dishes (D11530H MATSUNAMI) and incubated with medium containing 10 μmol/L Fluo-8 (21081 AAT Bioquest) at 37°C for 30 min. For the G-CaMP3 Method[63], a plasmid encoding G-CaMP3 was transfected into HeLa cells on coverslips and incubated for 30 min. For both methods, fluorescence images at 485 nm were acquired on SP-8. Fluorescence intensity inside the encircled ROI (5 μm in diameter) in the cytoplasmic region was measured using ImageJ. Calcium concentration was calculated as follows: $[Ca^{2+}]=K_d$(Fluo-8 or G-CaMP3)$\times(F-F_{min})/(F_{max}-F)$. The K_d of Fluo8 is 389 nM, and the K_d of G-CaMP3 is 345 nM. F is the fluorescence signal intensity. F_{max} is the fluorescence signal intensity measured under $[Ca^{2+}]$ maximum in the presence of 1 μM ionomycin (095-05831 Wako). F_{min} is the fluorescence signal intensity measured under $[Ca^{2+}]$ minimum in the presence of BAPTA-AM (0373124 Nacalai Tesque) in HBSS

(Hanks balanced salt solution, modified, H9394 Sigma-Aldrich) medium containing 10 mM HEPES (1 mol/l-HEPES Buffer Solution pH 7.1~7.5 17557-94 Nacalai Tesque).

Statistical analysis

Bar-graphs were drawn with Excel for the average and standard deviation of three experiments if associated. Box-and-whisker plots were drawn with R for Median (line) upper and lower quartiles (boxes) 1.5-interquartile range (whiskers). Unpaired two-tailed Student's t-test between two samples (ex. EBSS and EBSS plus TJ-35) using Excel and * denotes $p<0.05$.

Figures

Figure 1-1

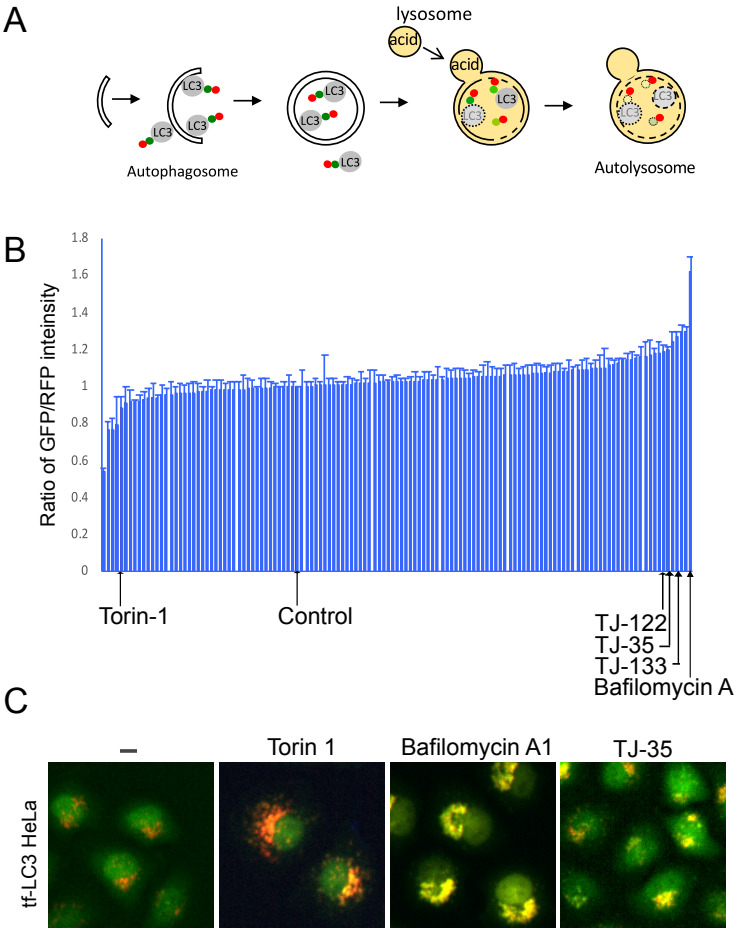

Fig 1-1. Screening for effects of Kampo on autophagy by tf-LC3 assay

A. Schematic diagram of tf-LC3 assay. **B**. Screening results of tf-LC3 assay upon treatment with 128 Kampo medicines. The signal intensity ratio of GFP/RFP in each view field after 24 h of incubation is presented in order of value. Average and standard deviation of three independent screenings are shown. Bafilomycin A_1 and Torin1 were used as controls. **C.** Representative images of each sample of B.

Figure 1-2

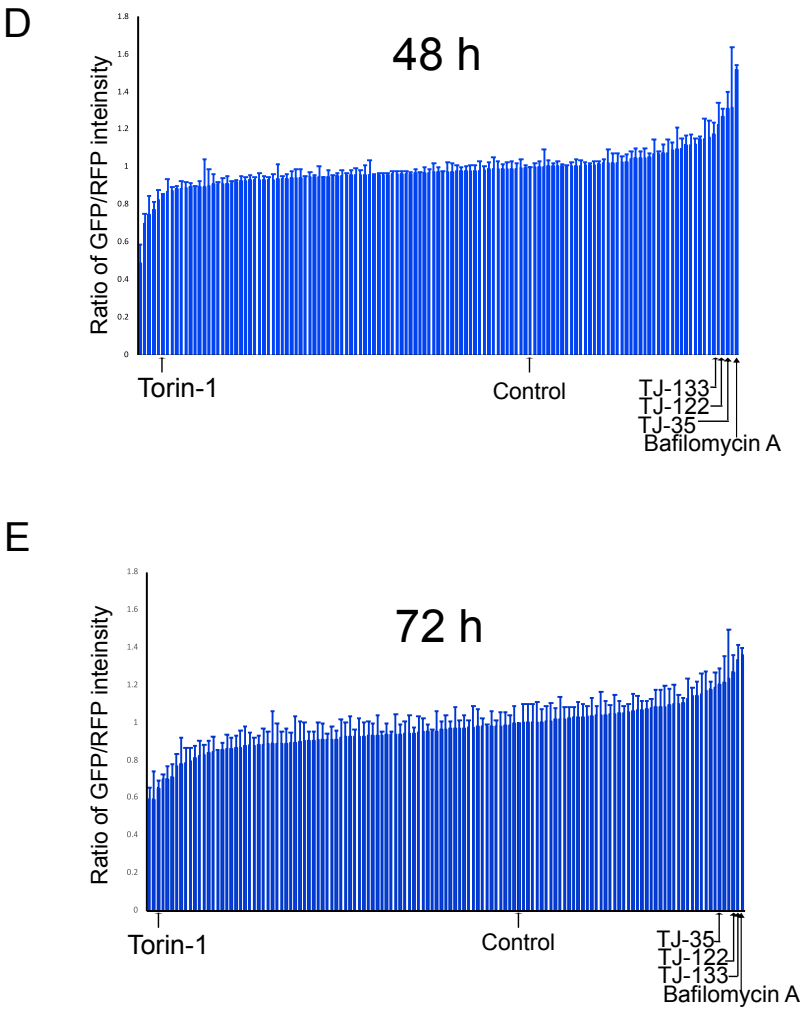

Fig 1-2. Screening for an effect of Kampo on autophagy by tf-LC3 assay

D.E. Screening results of tf-LC3 assay upon treatment with 128 Kampo medicines. The signal intensity ratio of GFP/RFP in each view field at 48 h (D) or 72 h (E) incubation is presented in order of its value. Average and standard deviation of three independent screens are shown. Bafilomycin A_1 and Torin-1 were used as controls.

Figure 2

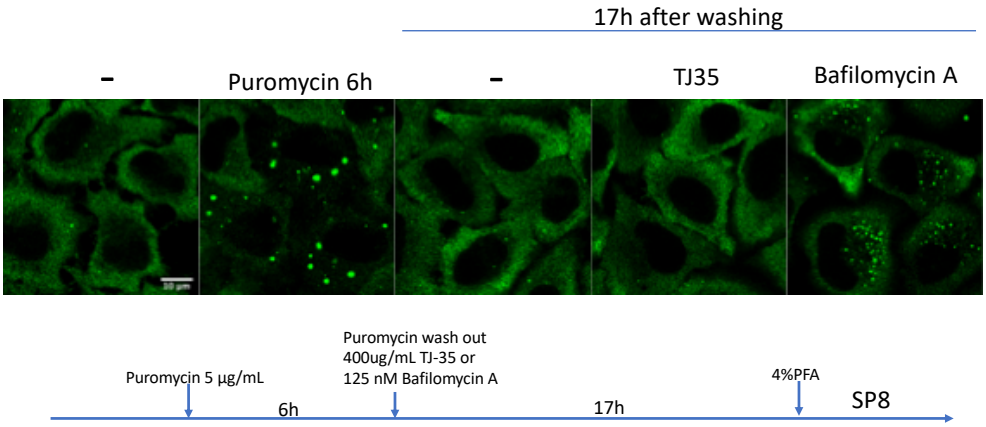

Fig 2. Assessment of an effect of TJ-35 on aggrephagy

HeLa cells were cultured in DMEM with or without puromycin for 6 h, and after being washed out, further cultured in DMEM with or without TJ-35 for 17 h and immunostained with anti-p62 on SP-8. Bafilomycin A_1 was used as controls.

Figure 3-1

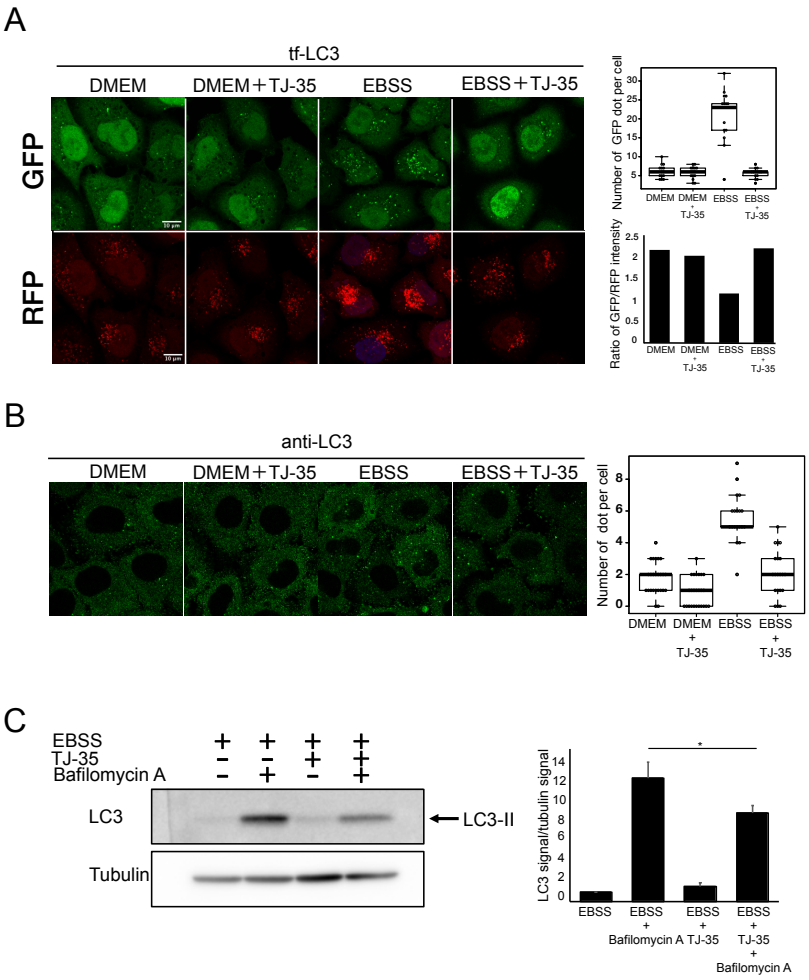

Fig 3-1. TJ-35 suppresses autophagy under starvation condition

A. Tf-LC3–expressing HeLa cells were treated with or without TJ35 for 4 h, shifted to DMEM or EBSS with or without TJ-35 for 2 h, and observed on SP-8. The graph above shows GFP-positive puncta per cell. Median: line; upper and lower quartiles: boxes; 1.5-interquartile range: whiskers. I counted 15 cells in three independent experiments. Bar represents 10 μm. The graph below shows the signal intensity ratio of GFP/RFP in each field of view after 6 h. **B**. HeLa cells were cultured in DMEM for 24 h, treated with or without TJ-35 for 4 h, and shifted to EBSS in the presence of TJ-35 for 2 h. The cells were immunostained with anti-LC3 antibody. The graph shows Alexa Fluor 488-positive puncta per cell. Median: line; upper and lower quartiles: boxes; 1.5-interquartile range: whiskers. I counted 25 cells in three independent experiments. Bar represents 10 μm. **C**. HeLa cells were treated with or without TJ35 in DMEM or EBSS, with or without bafilomycin A_1, for 4 h. The lysates were assessed by Western Blotting with LC3 antibody. The graph shows the average and standard deviation of LC3 signal versus tubulin signal from three independent experiments. * denotes $p<0.05$ (unpaired two-tailed Student's t-test) between EBSS and EBSS plus TJ-35.

Figure 3-2

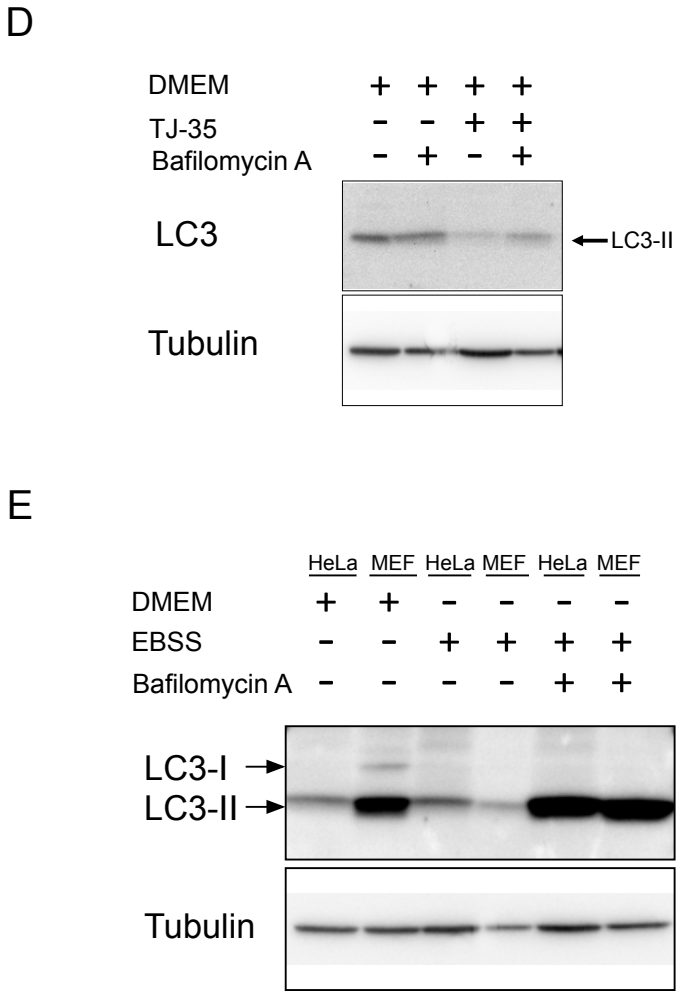

Fig. 3-2. TJ-35 suppresses autophagy under starvation condition

D. HeLa cells were treated with or without TJ35 in DMEM, with or without bafilomycin A_1, for 4 h. The lysates were assessed by Western Blotting with LC3 antibody. **E**. Comparison of Band pattern of LC3 by western blotting: MEF and HeLa cells were cultured in DMEM or EBSS, with or without bafilomycin A_1, for 4 h. The lysates were assessed by western blotting with antibodies against LC3 and tubulin

Figure 4

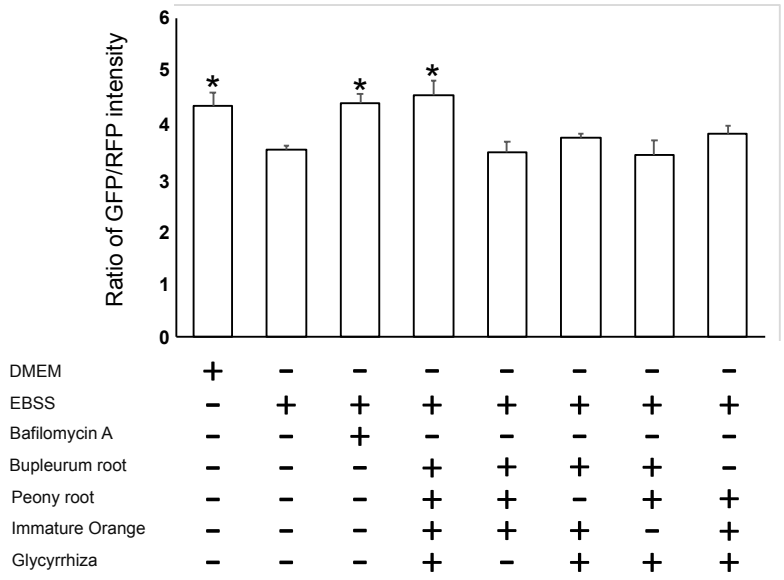

Fig 4. Analysis of TJ-35/Shigyakusan ingredients in autophagy

Tf-LC3–expressing HeLa cells were cultured in DMEM with or without Shigyakusan and with extracts with omission of any of the four crude drugs for 4 h, shifted to DMEM or EBSS with or without the above combination of Shigaykusan ingredients for 2 h, and observed on SP-8. The graph below shows the signal intensity ratio of GFP/RFP in each field of view. * denotes $p<0.05$ (unpaired two-tailed Student's t-test) against EBSS only sample.

Figure 5

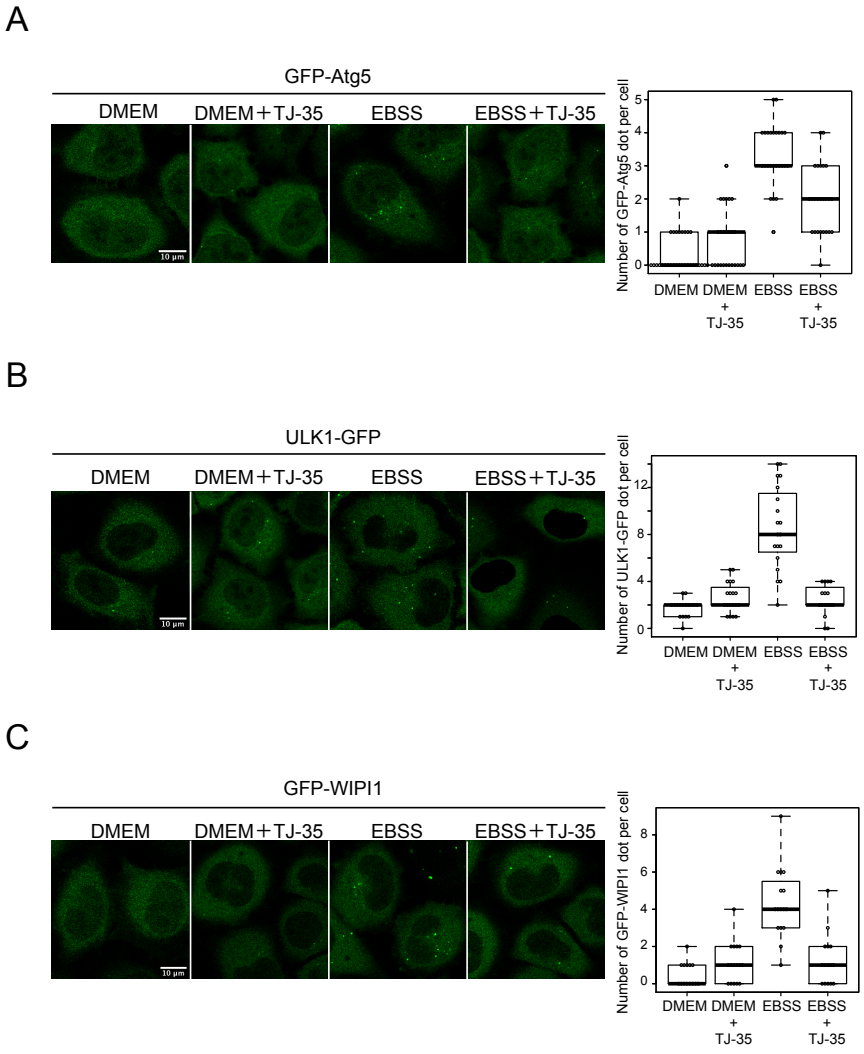

Fig 5. TJ-35 suppresses autophagosome formation under starvation condition

A. GFP-Atg5 expressing HeLa was treated with or without TJ-35 for 4 h, and then shifted to DMEM or EBSS with or without TJ-35 for 2 h. The graph shows GFP-positive puncta per cell. Median: line; upper and lower quartiles: boxes; 1.5-interquartile range: whiskers. I counted 25 cells in three independent experiments. Bar represents 10 μm. **B**. ULK1-EGFP expressing HeLa was treated with or without TJ-35 for 4 h and shifted to DMEM or EBSS with or without TJ-35 for 2 h. The graph shows GFP-positive puncta per cell. Median: line; upper and lower quartiles: boxes; 1.5-interquartile range: whiskers. I counted 25 cells in three independent experiments. Bar represents 10 μm. **C**. GFP-WIPI1–expressing HeLa cells were treated with or without TJ-35 for 4 h and shifted to DMEM or EBSS with or without TJ-35 for 2 h. The graph shows GFP-positive puncta per cell. Median: line; upper and lower quartiles: boxes; 1.5-interquartile range: whiskers. I counted 15 cells in three independent experiments. Bar represents 10 μm. * denotes $p<0.05$ (unpaired two-tailed Student's t-test) between EBSS and EBSS plus TJ-35.

Figure 6

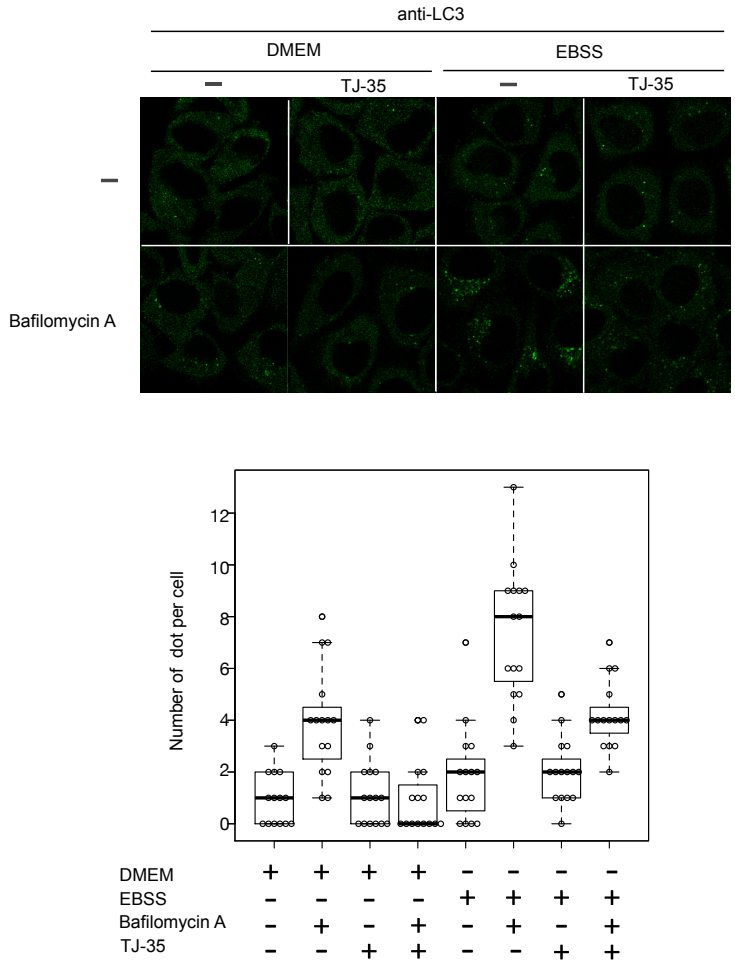

Fig 6. TJ-35 suppresses autophagosome formation under starvation condition

HeLa cells were treated with or without TJ35 in DMEM or EBSS, with or without bafilomycin A_1, for 4 h. The cells were immunostained with anti-LC3 antibody. The graph shows Alexa Fluor 488-positive puncta per cell. Median: line; upper and lower quartiles: boxes; 1.5-interquartile range: whiskers.

Figure 7

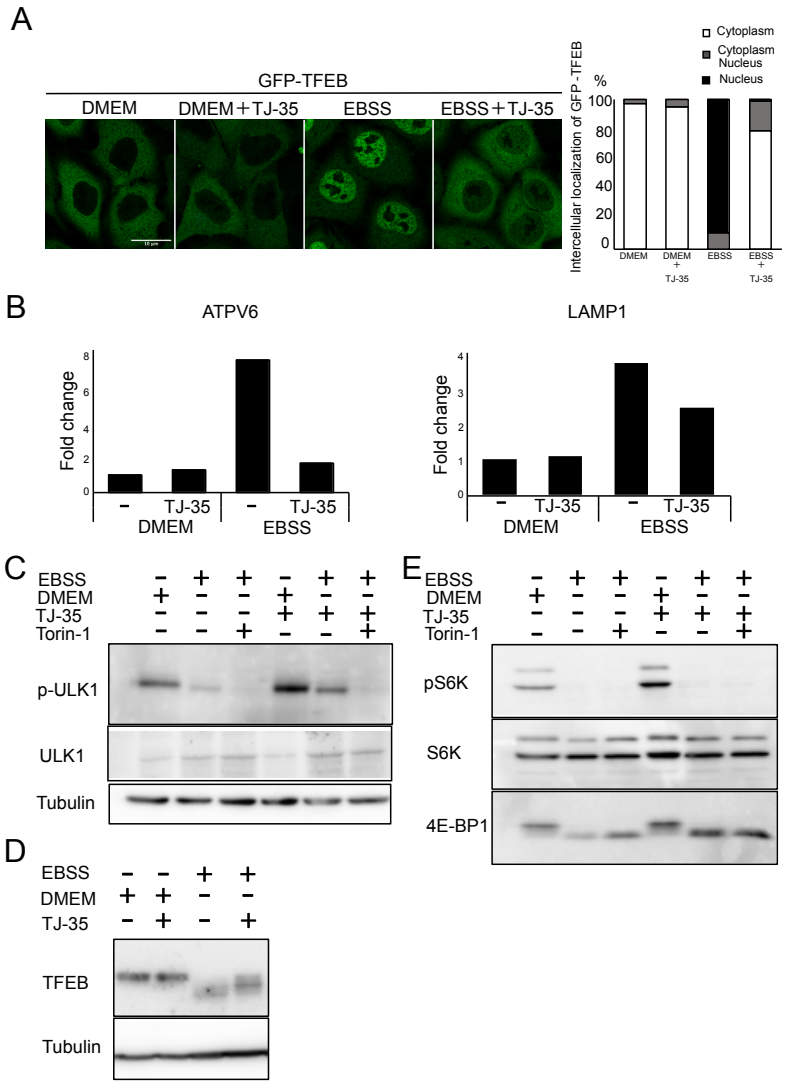

Fig 7. TJ-35 suppresses dephosphorylation of ULK1 and TFEB specifically among mTORC1 substrates

A. GFP-TFEB expressing HeLa cells were treated with or without TJ-35 for 4 h, and then shifted to DMEM or EBSS with or without TJ-35 for 2 h. Bar represents 10 μm. The graph shows quantification of GFP-TFEB that localized in the cytoplasm or nucleus. Percent of cells with cytoplasmic, nucleus or both. I counted 30 cells in three independent experiments. **B**. HeLa cells were treated with or without TJ-35 in DMEM or EBSS for 4 h, and then total RNA was extracted. Expression levels of ATPV6 and LAMP1 versus GAPDH were monitored by RT qPCR. The graph shows fold change. **CE**. HeLa cells were treated with or without TJ-35 for 4 h, shifted to DMEM or EBSS with or without TJ-35 or Torin-1 for 2 h, and then subjected to immunoblotting with anti-TFEB, anti-phosopho-S6K, anti-p70 kinase, anti-4E-BP1 and anti-Tubulin. The samples of C and E were derived from the same preparation. **D**. HeLa cells were treated with or without TJ-35 for 4 h, shifted to DMEM or EBSS with or without TJ-35 or Torin-1 for 2 h, and then subjected to immunoblotting with anti-phospho-ULK1(Ser757), anti-ULK1 and anti-Tubulin.

Figure 8-1

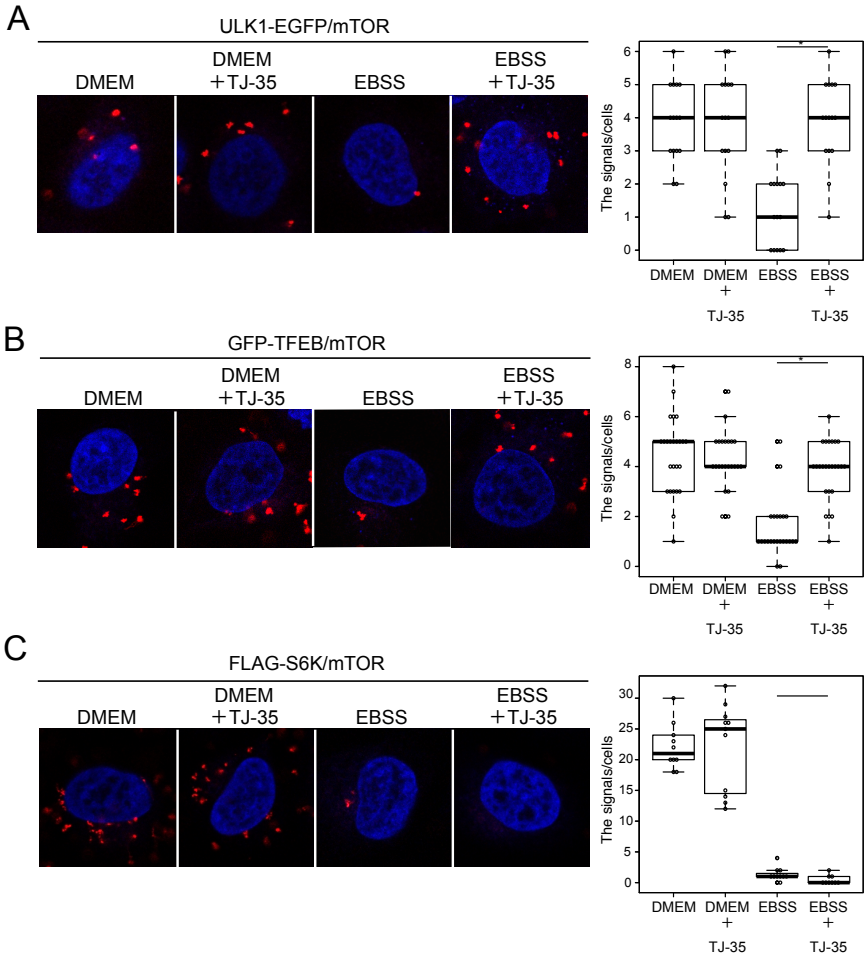

Fig 8-1. TJ-35 specifically suppresses dissociation of ULK1 and TFEB from mTORC1 under starvation conditions

A. ULK1-EGFP–expressing HeLa cells were treated with or without TJ-35 for 4 h, and shifted to DMEM or EBSS with or without TJ-35 for 2 h, and subjected to PLA using anti-GFP and mTOR antibodies. I counted 15 cells counted in two independent experiments. **B**. GFP-TFEB–expressing HeLa cells were treated with or without TJ-35 for 4 h, shifted to DMEM or EBSS with or without TJ-35 for 2 h, and subjected to PLA using anti-GFP and mTOR antibodies. I counted 30 cells in two independent experiments. **C**. FLAG-S6K–expressing HeLa was treated with TJ-35 for 4 h and shifted to DMEM or EBSS with or without TJ-35 for 2 h, and subjected to PLA using anti-FLAG and mTOR antibodies. I counted 10 cells in two independent experiments. * denotes $p<0.05$ (unpaired two-tailed Student's t-test) between EBSS and EBSS plus TJ-35.

Figure 8-2

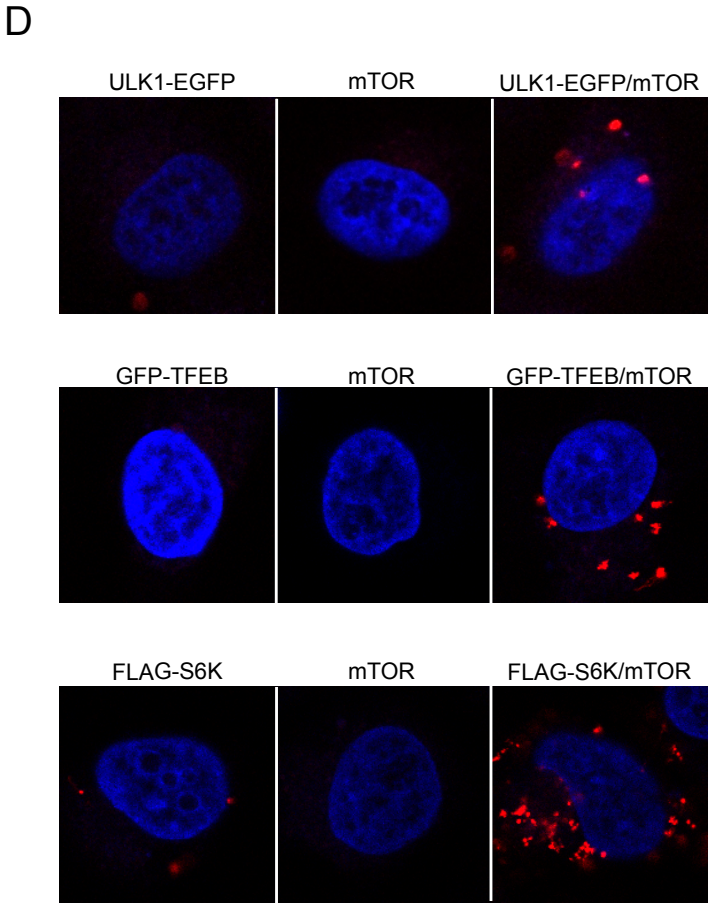

Fig 8-2. TJ-35 specifically suppresses dissociation of ULK1 and TFEB from mTORC1 under starvation conditions

D. ULK1-EGFP–expressing HeLa cells and GFP-TFEB–expressing HeLa were cultured in DMEM for 24 h, and subjected to PLA using either anti-GFP antibody or mTOR antibody or both. FLAG-S6K–expressing HeLa were cultured in DMEM for 24 h, and subjected to PLA using either anti-FLAG antibody or mTOR antibody or both.

Figure 9

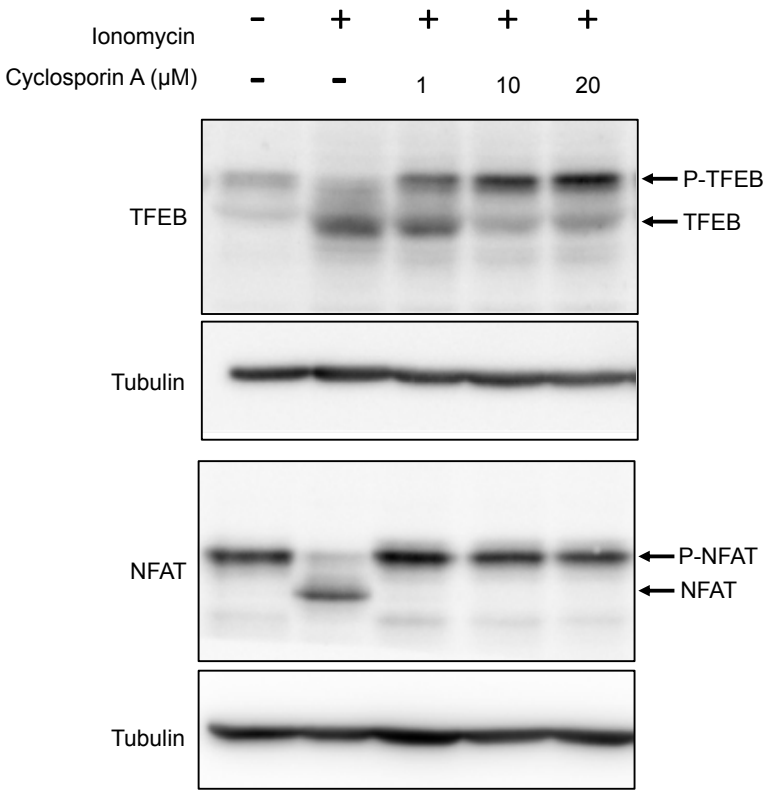

Fig 9. Cytosolic [Ca^{2+}] increment induces TFEB dephosphorylation via calcineurin

HeLa cells expressing HA-NFAT (Addgene: 11107) were treated with ionomycin in DMEM for 1 h with or without the indicated concentration of cyclosporin A. Lysates were immunoblotted with anti-TFEB and anti-HA.

Figure 10

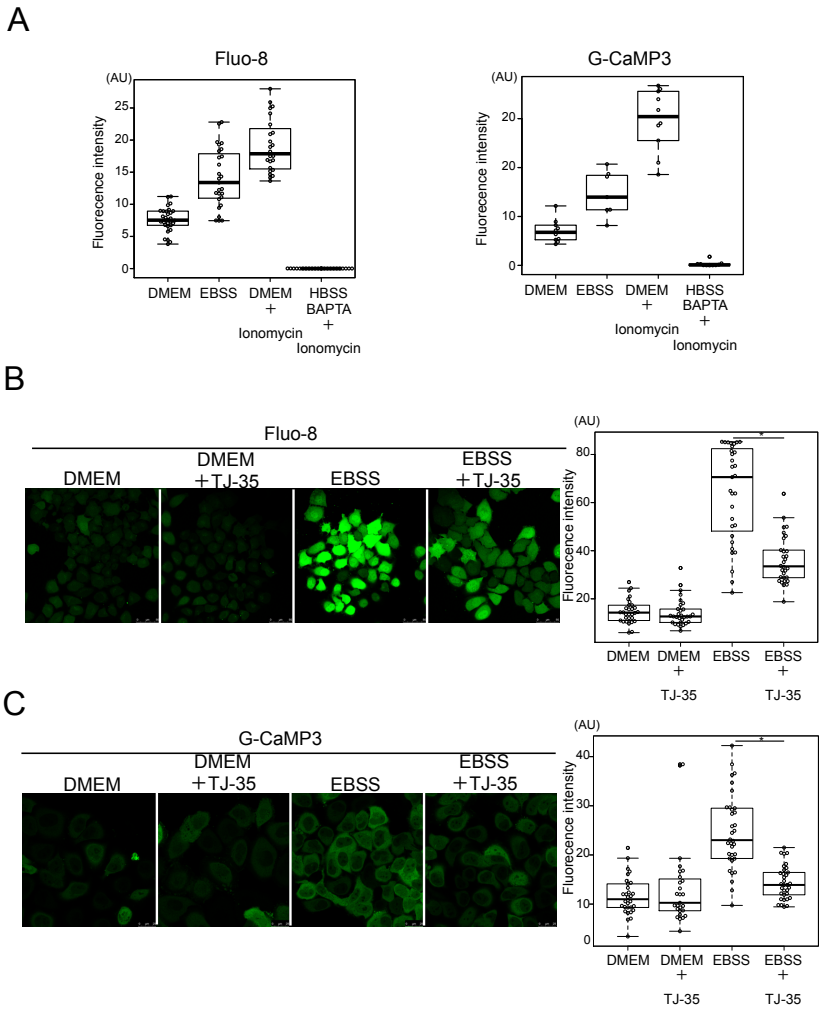

Fig 10. TJ-35 suppresses cytosolic Ca^{2+} increment under starvation condition

A. HeLa cells were cultured with DMEM for 24 h, shifted to EBSS for 2 h. The cells were stained with Fluo-8 for 30 min. HeLa cells were transiently transfected with G-CaMP3 (Addgene: 22692) for 24 h, and shifted to EBSS for 2 h. For measuring Fmax, ionomycin was added to DMEM. For measuring Fmin, HeLa cells transiently transfected with G-CaMP3 were cultured and added ionomycin with BAPTA in HBSS. **B**. HeLa cells were cultured with DMEM for 24 h, shifted to EBSS with or without TJ-35. The cells were stained with Fluo-8 for 30 min. I counted 30 cells in three independent experiments. **C**. HeLa cells were transiently transfected with G-CaMP3 for 24 h, shifted to EBSS with or without TJ-35. I counted 30 cells in three independent experiments. **ABC**. Fluorescence intensity in ROI within cytoplasm was measured. Median: line; upper and lower quartiles: boxes; 1.5-interquartile range: whiskers. * denotes $p<0.05$ (unpaired two-tailed Student's t-test) between EBSS and EBSS plus TJ-35.

Figure 11

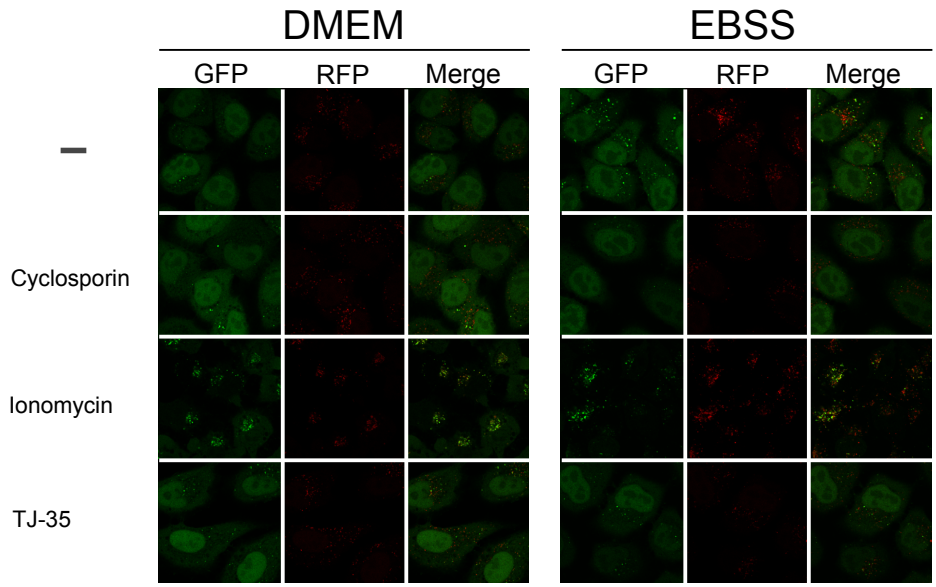

Fig 11. Ca^{2+} **increment induces autophagy and calcineurin inhibitor suppresses autophagy**
Tf-LC3–expressing HeLa cells were treated in DMEM or EBSS with 3 μM ionomycin or 20 μM cyclosporin A for 30 min. TJ-35 treatment condition was the same as above. Images were acquired on SP-8.

Figure 12

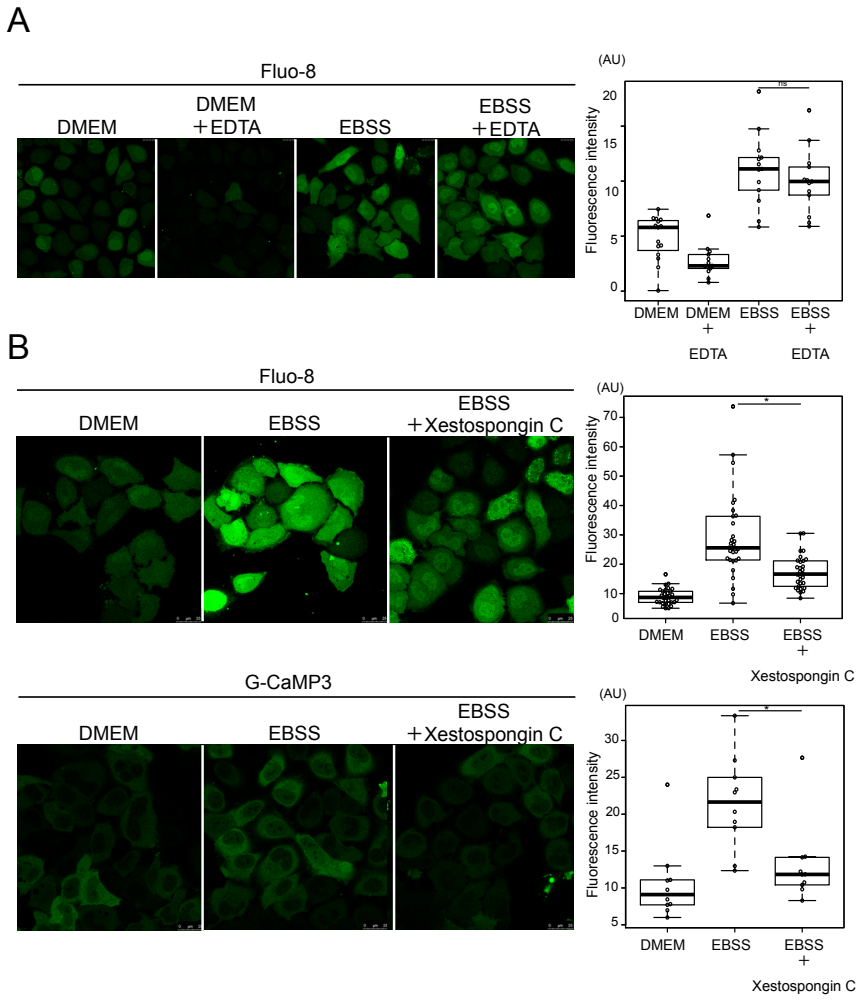

Fig 12. Starvation induced calcium efflux from the ER mediated by the IP3 receptor

A. HeLa cells were cultured with 0.5 mM EDTA in EBSS for 90 min and then stained with Fluo-8 for 30 min. 15 cells were counted in three independent experiments. **B**. HeLa cells were treated with or without xestospongin C in DMEM or EBSS for 90 min, and then stained with Fluo-8 for 30 min. 15 cells were counted in three independent experiments. HeLa cells were transiently transfected with G-CaMP3 and shifted to DMEM or EBSS with or without xestospongin C for 2 h. 30 cells were counted in three independent experiments. Fluorescence intensity was measured in ROI within cytoplasm. Median: line; upper and lower quartiles: boxes; 1.5-interquartile range: whiskers. * denotes $p<0.05$ (unpaired two-tailed Student's t-test) between EBSS and EBSS plus drug treatment

Figure 13

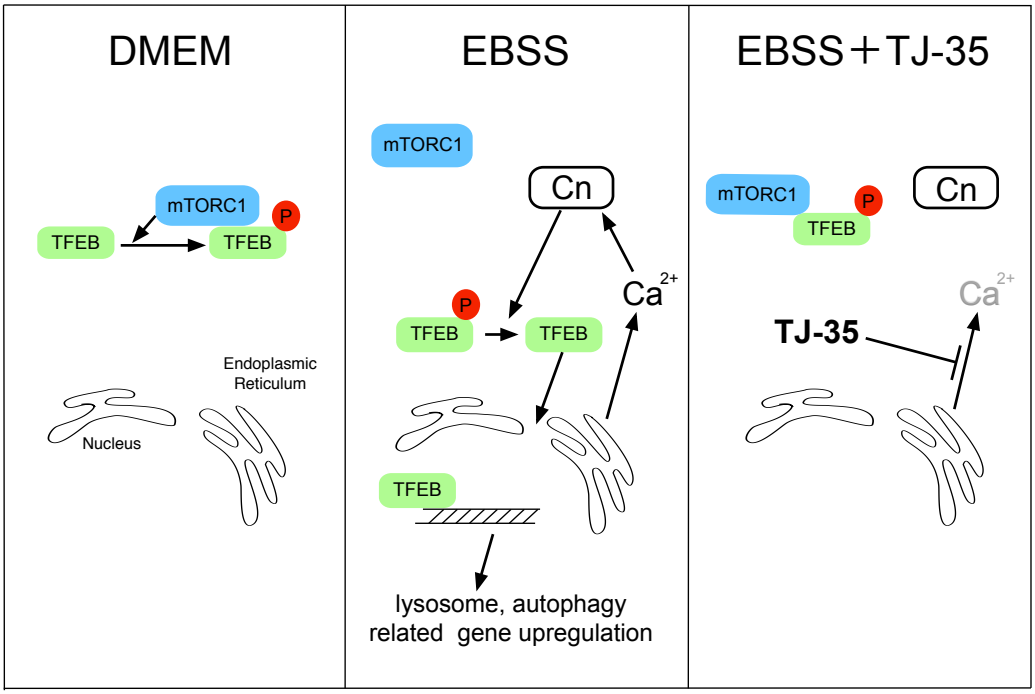

Fig 13. Model of the mechanism of effects of Shigyakusan to suppress starvation-induced autophagy via calcium -dependent TFEB dephosphorylation

Under nutrient rich conditions, mTORC1 and TFEB are bound, and TFEB is phosphorylated by mTORC1 in the cytoplasm. Under starvation conditions, cytosolic calcium increases and the calcineurin substrate TFEB is dephosphorylated. Dephosphorylated TFEB translocases into the nucleus and contributes as a transcription factor to the expression of lysosome and autophagy-related gene.

The effects of TJ-35 suppressed cytosolic calcium under starvation conditions. Starvation-induced autophagy via calcium0dependent TFEB dephosphorylation is suppressed by Shigyakusan (TJ-35)

Figures Legends

Fig 1. Screening for effects of Kampo on autophagy by tf-LC3 assay

A. Schematic diagram of tf-LC3 assay. **B**. Screening results of tf-LC3 assay upon treatment with 128 Kampo medicines. The signal intensity ratio of GFP/RFP in each view field after 24 h of incubation is presented in order of value. Average and standard deviation of three independent screenings are shown. Bafilomycin A_1 and Torin1 were used as controls. **C.** Representative images of each sample of B. **D.E.** Screening results of tf-LC3 assay upon treatment with 128 Kampo medicines. The signal intensity ratio of GFP/RFP in each view field at 48 h (D) or 72 h (E) incubation is presented in order of its value. Average and standard deviation of three independent screens are shown. Bafilomycin A_1 and Torin-1 were used as controls.

Fig 2. Assessment of an effect of TJ-35 on aggrephagy

HeLa cells were cultured in DMEM with or without puromycin for 6 h, and after being washed out, further cultured in DMEM with or without TJ-35 for 17 h, and immunostained with anti-p62 on SP-8.

Fig 3-1. TJ-35 suppresses autophagy under starvation condition

A. Tf-LC3–expressing HeLa cells were treated with or without TJ35 for 4 h, shifted to DMEM or EBSS with or without TJ-35 for 2 h, and observed on SP-8. The graph above shows GFP-positive puncta per cell. Median: line; upper and lower quartiles: boxes; 1.5-interquartile range: whiskers. I counted 15 cells in three independent experiments. Bar represents 10 μm. The graph below shows the signal intensity ratio of GFP/RFP in each field of view after 6 h. **B**. HeLa cells were cultured in

DMEM for 24 h, treated with or without TJ-35 for 4 h, and shifted to EBSS in the presence of TJ-35 for 2 h. The cells were immunostained with anti-LC3 antibody. The graph shows Alexa Fluor 488-positive puncta per cell. Median: line; upper and lower quartiles: boxes; 1.5-interquartile range: whiskers. I counted 25 cells in three independent experiments. Bar represents 10 μm. **C**. HeLa cells were treated with or without TJ35 in DMEM or EBSS, with or without bafilomycin A_1, for 4 h. The lysates were assessed by Western Blotting with LC3 antibody. The graph shows the average and standard deviation of LC3 signal versus tubulin signal from three independent experiments. * denotes $p<0.05$ (unpaired two-tailed Student's t-test) between EBSS and EBSS plus TJ-35. **D**. HeLa cells were treated with or without TJ35 in DMEM, with or without bafilomycin A_1, for 4 h. The lysates were assessed by Western Blotting with LC3 antibody. **E**. Comparison of Band pattern of LC3 by western blotting: MEF and HeLa cells were cultured in DMEM or EBSS, with or without bafilomycin A_1, for 4 h. The lysates were assessed by western blotting with antibodies against LC3 and tubulin

Fig 4. Analysis of TJ-35/Shigyakusan ingredients in autophagy

Tf-LC3–expressing HeLa cells were cultured in DMEM with or without Shigyakusan and with extracts with omission of any of the four crude drugs for 4 h, shifted to DMEM or EBSS with or without the above combination of Shigaykusan ingredients for 2 h, and observed on SP-8. The graph below shows the signal intensity ratio of GFP/RFP in each field of view. * denotes $p<0.05$ (unpaired two-tailed Student's t-test) against EBSS only sample.

Fig 5. TJ-35 suppresses autophagosome formation under starvation condition

A. GFP-Atg5 expressing HeLa was treated with or without TJ-35 for 4 h, and then shifted to DMEM or EBSS with or without TJ-35 for 2 h. The graph shows GFP-positive puncta per cell. Median: line; upper and lower quartiles: boxes; 1.5-interquartile range: whiskers. I counted 25 cells in three independent experiments. Bar represents 10 μm. **B**. ULK1-EGFP expressing HeLa was treated with or without TJ-35 for 4 h and shifted to DMEM or EBSS with or without TJ-35 for 2 h. The graph shows GFP-positive puncta per cell. Median: line; upper and lower quartiles: boxes; 1.5-interquartile range: whiskers. I counted 25 cells in three independent experiments. Bar represents 10 μm. **C**. GFP-WIPI1–expressing HeLa cells were treated with or without TJ-35 for 4 h and shifted to DMEM or EBSS with or without TJ-35 for 2 h. The graph shows GFP-positive puncta per cell. Median: line; upper and lower quartiles: boxes; 1.5-interquartile range: whiskers. I counted 15 cells in three independent experiments. Bar represents 10 μm. * denotes $p<0.05$ (unpaired two-tailed Student's t-test) between EBSS and EBSS plus TJ-35.

Fig 6. TJ-35 suppresses autophagosome formation under starvation condition

HeLa cells were treated with or without TJ35 in DMEM or EBSS, with or without bafilomycin A_1, for 4 h. The cells were immunostained with anti-LC3 antibody. The graph shows Alexa Fluor 488-positive puncta per cell. Median: line; upper and lower quartiles: boxes; 1.5-interquartile range: whiskers.

Fig 7. TJ-35 suppresses dephosphorylation of ULK1 and TFEB specifically among mTORC1 substrates

A. GFP-TFEB expressing HeLa cells were treated with or without TJ-35 for 4 h, and then shifted to DMEM or EBSS with or without TJ-35 for 2 h. Bar represents 10 μm. The graph shows quantification of GFP-TFEB that localized in the cytoplasm or nucleus. Percent of cells with cytoplasmic, nucleus or both. I counted 30 cells in three independent experiments. **B**. HeLa cells were treated with or without TJ-35 in DMEM or EBSS for 4 h, and then total RNA was extracted. Expression levels of ATPV6 and LAMP1 versus GAPDH were monitored by RT qPCR. The graph shows fold change. **CE**. HeLa cells were treated with or without TJ-35 for 4 h, shifted to DMEM or EBSS with or without TJ-35 or Torin-1 for 2 h, and then subjected to immunoblotting with anti-TFEB, anti-phosopho-S6K, anti-p70 kinase, anti-4E-BP1 and anti-Tubulin. The samples of C and E were derived from the same preparation. **D**. HeLa cells were treated with or without TJ-35 for 4 h, shifted to DMEM or EBSS with or without TJ-35 or Torin-1 for 2 h, and then subjected to immunoblotting with anti-phospho-ULK1(Ser757), anti-ULK1 and anti-Tubulin.

Fig 8. TJ-35 specifically suppresses dissociation of ULK1 and TFEB from mTORC1 under starvation conditions

A. ULK1-EGFP–expressing HeLa cells were treated with or without TJ-35 for 4 h, and shifted to DMEM or EBSS with or without TJ-35 for 2 h, and subjected to PLA using anti-GFP and mTOR antibodies. I counted 15 cells counted in two independent experiments. **B**. GFP-TFEB–expressing HeLa cells were treated with or without TJ-35 for 4 h, shifted to DMEM or EBSS with or without TJ-35 for 2 h, and subjected to PLA using anti-GFP and mTOR antibodies. I counted 30 cells in two independent experiments. C. FLAG-S6K–expressing HeLa was treated with TJ-35 for 4 h and shifted

to DMEM or EBSS with or without TJ-35 for 2 h, and subjected to PLA using anti-FLAG and mTOR antibodies. I counted 10 cells in two independent experiments. * denotes $p<0.05$ (unpaired two-tailed Student's t-test) between EBSS and EBSS plus TJ-35.

Fig 9. Cytosolic [Ca^{2+}] increment induces TFEB dephosphorylation via calcineurin

HeLa cells expressing HA-NFAT (Addgene: 11107) were treated with ionomycin in DMEM for 1 h with or without the indicated concentration of cyclosporin A. Lysates were immunoblotted with anti-TFEB and anti-HA.

Fig 10. TJ-35 suppresses cytosolic Ca^{2+} increment under starvation condition

A. HeLa cells were cultured with DMEM for 24 h, shifted to EBSS for 2 h. The cells were stained with Fluo-8 for 30 min. HeLa cells were transiently transfected with G-CaMP3 (Addgene: 22692) for 24 h, and shifted to EBSS for 2 h. For measuring Fmax, ionomycin was added to DMEM. For measuring Fmin, HeLa cells transiently transfected with G-CaMP3 were cultured and added ionomycin with BAPTA in HBSS. **B**. HeLa cells were cultured with DMEM for 24 h, shifted to EBSS with or without TJ-35. The cells were stained with Fluo-8 for 30 min. I counted 30 cells in three independent experiments. **C**. HeLa cells were transiently transfected with G-CaMP3 for 24 h, shifted to EBSS with or without TJ-35. I counted 30 cells in three independent experiments. **ABC**. Fluorescence intensity in ROI within cytoplasm was measured. Median: line; upper and lower quartiles: boxes; 1.5-interquartile range: whiskers. * denotes $p<0.05$ (unpaired two-tailed Student's t-test) between EBSS and EBSS plus TJ-35.

Fig 11. Ca^{2+} **increment induces autophagy and calcineurin inhibitor suppresses autophagy**

Tf-LC3–expressing HeLa cells were treated in DMEM or EBSS with 3 μM ionomycin or 20 μM cyclosporin A for 30 min. TJ-35 treatment condition was the same as above. Images were acquired on SP-8.

Fig 12. Starvation induced calcium efflux from the ER mediated by the IP3 receptor

A. HeLa cells were cultured with 0.5 mM EDTA in EBSS for 90 min and then stained with Fluo-8 for 30 min. 15 cells were counted in three independent experiments. **B**. HeLa cells were treated with or without xestospongin C in DMEM or EBSS for 90 min, and then stained with Fluo-8 for 30 min. 15 cells were counted in three independent experiments. HeLa cells were transiently transfected with G-CaMP3 and shifted to DMEM or EBSS with or without xestospongin C for 2 h. 30 cells were counted in three independent experiments. Fluorescence intensity was measured in ROI within cytoplasm. Median: line; upper and lower quartiles: boxes; 1.5-interquartile range: whiskers. * denotes $p<0.05$ (unpaired two-tailed Student's t-test) between EBSS and EBSS plus drug treatment

Fig 13. Model of the mechanism of effects of Shigyakusan to suppress starvation-induced autophagy via calcium -dependent TFEB dephosphorylation

Under nutrient rich conditions, mTORC1 and TFEB are bound, and TFEB is phosphorylated by mTORC1 in the cytoplasm. Under starvation conditions, cytosolic calcium increases and the calcineurin substrate TFEB is dephosphorylated. Dephosphorylated TFEB translocases into the

nucleus and contributes as a transcription factor to the expression of lysosome and autophagy-related gene. The effects of TJ-35 suppressed cytosolic calcium. Starvation-induced autophagy via calcium0dependent TFEB dephosphorylation is suppressed by Shigyakusan(TJ-35)

References

1. Takeshige K, Baba M, Tsuboi S, Noda T, Ohsumi Y. Autophagy in yeast demonstrated with proteinase-deficient mutants and conditions for its induction. J Cell Biol. 1992;119: 301–312. doi:10.1083/jcb.119.2.301

2. Baba M, Takeshige K, Baba N, Ohsumi Y. Ultrastructural analysis of the autophagic process in yeast: Detection of autophagosomes and their characterization. J Cell Biol. 1994;124: 903–913. doi:10.1083/jcb.124.6.903

3. Noda T, Ohsumi Y. Tor, a phosphatidylinositol kinase homologue, controls autophagy in yeast. J Biol Chem. 1998;273: 3963–3966. doi:10.1074/jbc.273.7.3963

4. Onodera J, Ohsumi Y. Autophagy is required for maintenance of amino acid levels and protein synthesis under nitrogen starvation. J Biol Chem. 2005;280: 31582–31586. doi:10.1074/jbc.M506736200

5. Takahashi Y, Liang X, Hattori T, Tang Z, He H, Chen H, Liu X, Abraham T, Imamura-Kawasawa Y, Buchkovich NJ, Young MM, Wang HG. VPS37A directs ESCRT recruitment for phagophore closure. J Cell Biol. 2019;218: 3336–3354. doi:10.1083/jcb.201902170

6. Matsuura A, Tsukada M, Wada Y, Ohsumi Y. Apg1p, a novel protein kinase required for the autophagic process in Saccharomyces cerevisiae. Gene. 1997;192: 245–250. doi:10.1016/S0378-1119(97)00084-X

7. Nakatogawa H, Suzuki K, Kamada Y, Ohsumi Y. Dynamics and diversity in autophagy mechanisms: Lessons from yeast. Nat Rev Mol Cell Biol. 2009;10: 458–467. doi:10.1038/nrm2708

8. Yoshimori T. Autophagy: A regulated bulk degradation process inside cells. Biochem Biophys Res Commun. 2004;313: 453–458. doi:10.1016/j.bbrc.2003.07.023

9. Kamada Y, Yoshino K, Kondo C, Kawamata T, Oshiro N, Yonezawa K, Ohsumi Y. Tor Directly Controls the Atg1 Kinase Complex To Regulate Autophagy. Mol Cell Biol. 2010;30: 1049–1058. doi:10.1128/mcb.01344-09

10. Kabeya Y, Kawamata T, Suzuki K, Ohsumi Y. Cis1/Atg31 is required for autophagosome formation in Saccharomyces cerevisiae. Biochem Biophys Res Commun. 2007;356: 405–410. doi:10.1016/j.bbrc.2007.02.150

11. Kametaka S, Okano T, Ohsumi M, Ohsumi Y. Apg14p and Apg6/Vps30p form a protein complex essential for autophagy in the yeast, Saccharomyces cerevisiae. J Biol Chem. 1998;273: 22284–22291. doi:10.1074/jbc.273.35.22284

12. Noda T, Kim J, Huang WP, Baba M, Tokunaga C, Ohsumi Y, Klionsky DJ. Apg9p/Cvt7p is an integral membrane protein required for transport vesicle formation in the Cvt and autophagy pathways. J Cell Biol. 2000;148: 465–479. doi:10.1083/jcb.148.3.465

13. Reggiori F, Klionsky DJ. Atg9 sorting from mitochondria is impaired in early secretion and VFT-complex mutants in Saccharomyces cerevisiae. J Cell Sci. 2006;119: 2903–2911. doi:10.1242/jcs.03047

14. Kabeya Y, Mizushima N, Yamamoto A, Oshitani-Okamoto S, Ohsumi Y, Yoshimori T. LC3, GABARAP and GATE16 localize to autophagosomal membrane depending on form-II formation. J Cell Sci. 2004;117: 2805–2812. doi:10.1242/jcs.01131

15. Tanida I, Tanida-Miyake E, Ueno T, Kominami E. The human homolog of Saccharomyces cerevisiae Apg7p is a protein-activating enzyme for multiple substrates including human Apg12p, GATE-16, GABARAP, and MAP-LC3. J Biol Chem. 2001;276: 1701–1706. doi:10.1074/jbc.C000752200

16. Tanida I, Tanida-Miyake E, Komatsu M, Ueno T, Kominami E. Human Apg3p/Aut1p homologue is an authentic E2 enzyme for multiple substrates, GATE-16, GABARAP, and MAP-LC3, and facilitates the conjugation of hApg12p to hApg5p. J Biol Chem. 2002;277: 13739–13744. doi:10.1074/jbc.M200385200

17. Mizushima N, Noda T, Yoshimori T, Tanaka Y, Ishii T, George MD, Klionsky DJ, Ohsumi Y. A protein conjugation system essential for autophagy. Nature. 1998;395: 395–398. doi:10.1038/26506

18. Ichimura Y, Kirisako T, Takao T, Satomi Y, Shimonishi Y, Ishihara N, Mizushima N, Tanida I, Kominami E, Ohsumi M, Noda T, Ohsumi Y. A ubiquitin-like system mediates protein lipidation. Nature. 2000;408: 488–492. doi:10.1038/35044114

19. Ranik J Xavier and John D Rioux. Genome-wide association studies: a new window into immune- mediated diseases. Nat Rev Immunol. 2008;8: 631–643. doi:10.1038/nri2361.

20. Saitoh T, Fujita N, Jang MH, Uematsu S, Yang BG, Satoh T, Omori H, Noda T, Yamamoto N, Komatsu M, Tanaka K, Tsujimura T, Takeuchi O, Yoshimori T, Akira S. Loss of the autophagy protein Atg16L1 enhances endotoxin-induced IL-1β production. Nature. 2008;456: 264–268. doi:10.1038/nature07383

21. Narendra D, Tanaka A, Suen DF, Youle RJ. Parkin is recruited selectively to impaired mitochondria and promotes their autophagy. J Cell Biol. 2008;183: 795–803. doi:10.1083/jcb.200809125

22. Durcan TM, Fon EA. The three 'P's of mitophagy: PARKIN, PINK1, and post-translational modifications. Genes Dev. 2015;29: 989–999. doi:10.1101/gad.262758.115.GENES

23. Ohba C, Nabatame S, Iijima Y, Nishiyama K, Tsurusaki Y, Nakashima M, Miyake N, Tanaka F, Ozono K, Saitsu H, Matsumoto N. De novo WDR45 mutation in a patient showing clinically Rett syndrome with childhood iron deposition in brain. J Hum Genet. 2014;59: 292–295. doi:10.1038/jhg.2014.18

24. Jiang P, Mizushima N. Autophagy and human diseases. Cell Res. 2014;24: 69–79. doi:10.1038/cr.2013.161

25. 日本漢方生薬製剤協会．漢方薬処方実態調査（定量）Summary Report．2011. https://www.nikkankyo.org/serv/pdf/jittaichousa2011.pdf

26. Okamoto H, Iyo M, Ueda K, Han C, Hirasaki Y, Namiki T. Yokukan-san: A review of the evidence for use of this Kampo herbal formula in dementia and psychiatric conditions. Neuropsychiatr Dis Treat. 2014;10: 1727–1742. doi:10.2147/NDT.S65257

27. Fujitsuka N, Uezono Y. Rikkunshito, a ghrelin potentiator, ameliorates anorexia-cachexia syndrome. Front Pharmacol. 2014;5: 1–9. doi:10.3389/fphar.2014.00271

28. Yasunaga H, Miyata H, Horiguchi H, Kuwabara K, Hashimoto H, Matsuda S. Effect of the Japanese herbal kampo medicine Dai-kenchu-to on postoperative adhesive small bowel obstruction requiring long-tube decompression: A propensity score analysis. Evidence-based Complement Altern Med. 2011; Volume 2011. Article ID 264289. doi:10.1155/2011/264289

29. Mizushima N. A brief history of autophagy from cell biology to physiology and disease. Nat Cell Biol. 2018;20: 521–527. doi:10.1038/s41556-018-0092-5

30. Zhao YG, Zhang H. Core autophagy genes and human diseases. Curr Opin Cell Biol. 2019;61: 117–125. doi:10.1016/j.ceb.2019.08.003

31. Luo T, Fu J, Xu A, Su B, Ren Y, Li N, Zhu J, Zhao X, Dai R, Cao J, Qin W, Jlang J, Li J, Wu M, Feng G, Chen Y, Wang H. PSMD10/gankyrin induces autophagy to promote tumor progression through cytoplasmic interaction with ATG7 and nuclear transactivation of ATG7 expression. Autophagy. 2016;12: 1355–1371. doi:10.1080/15548627.2015.1034405

32. Liu M, Jiang L, Fu X, Wang W, Ma J, Tian T,Nan K, Liang X. Cytoplasmic liver kinase B1 promotes the growth of human lung adenocarcinoma by enhancing autophagy. Cancer Sci. 2018;109: 3055–3067. doi:10.1111/cas.13746

33. Kinsey CG, Camolotto SA, Boespflug AM, Guillen KP, Foth M, Truong A, Schuman SS, Shea JE, Seipp MT, Yap JT, Burrell LD, Lum DH, Whisenant JR, Gllcrease GW 3rd, Cavalieri CC, Rehbein KM, Cutier SL, Affolter KE, Welm BE, Scaife CL, Snyder EL, Mcmahon M. Protective autophagy elicited by RAF→MEK→ERK inhibition suggests a treatment strategy for RAS-driven cancers. Nat Med. 2019;25: 620–627. doi:10.1038/s41591-019-0367-9

34. Yusuf IH, Sharma S, Luqmani R, Downes SM. Hydroxychloroquine retinopathy. Eye. 2017;31: 828–845. doi:10.1038/eye.2016.298

35. Guido Kroemer. Autophagy : a druggable process that is deregulated in aging and hum an disease. J Clin Invest. 2015;125: 1–5. doi:10.1172/JCI78652.oncogenesis

36. Rubinsztein DC, Codogno P, Levine B. Autophagy modulation as a potential therapeutic target for diverse diseases. Nat Rev Drug Discov. 2012;11: 709–730. doi:10.1038/nrd3802.Autophagy

37. Wang SF, Wu MY, Cai CZ, Li M, Lu JH. Autophagy modulators from traditional Chinese medicine: Mechanisms and therapeutic potentials for cancer and neurodegenerative diseases. J Ethnopharmacol. 2016;194: 861–876. doi:10.1016/j.jep.2016.10.069

38. Yu F, Takahashi T, Moriya J, Kawaura K, Yamakawa J, Kusaka K, Itoh T, Morimoto S, Yamaguchi N, Kanda T. Traditional Chinese medicine and kampo: A review from the distant past for the future. J Int Med Res. 2006;34: 231–239. doi:10.1177/147323000603400301

39. Takanashi K, Dan K, Kanzaki S, Hasegawa H, Watanabe K, Ogawa K. The Preventive Effect of the Traditional Japanese Herbal Medicine , Hochuekkito , against Influenza A Virus via Autophagy in vitro. Phamacology. 2019;99: 2017–2020.

40. Okubo S, Komori H, Kuwahara A, Ohta T, Shoyama Y, Uto T. Screening of Crude Drugs Used in Japanese Kampo Formulas for Autophagy-Mediated Cell Survival of the Human Hepatocellular Carcinoma Cell Line. Medicines. 2019;6: 63. doi:10.3390/medicines6020063

41. Kimura S, Fujita N, Noda T, Yoshimori T. Monitoring Autophagy in Mammalian Cultured Cells through the Dynamics of LC3. Method in Enzymology. 2009; 452:1-12. doi:10.1016/S0076-6879 (08)03601-X.

42. Kimura S, Noda T, Yoshimori T. Dissection of the autophagosome maturation process by a novel reporter protein, tandem fluorescent-tagged LC3. Autophagy. 2007;3: 452–460. doi:10.4161/auto.4451

43. Thoreen CC, Kang SA, Chang JW, Liu Q, Zhang J, Gao Y, Reichling LJ, Sim T, Sabatini DM, Gray NS. An ATP-competitive mammalian target of rapamycin inhibitor reveals rapamycin-resistant functions of mTORC1. J Biol Chem. 2009;284: 8023–8032. doi:10.1074/jbc.M900301200

44. Yamamoto A, Tagawa Y, Yoshimori T, Moriyama Y, Masaki R, Tashiro Y. Bafilomycin Ai Prevents Maturation of Autophagic Vacuoles by Inhibiting Fusion between Autophagosomes and Lysosomesin Rat Hepatoma Cell Line. Cell Struct Funct. 1998;23: 33–42.

45. Lamark T, Johansen T. Aggrephagy: Selective disposal of protein aggregates by macroautophagy. Int J Cell Biol. 2012;Volume 2012. Article ID 736905. doi:10.1155/2012/736905

46. Lippai M, Low P. The role of the selective adaptor p62 and ubiquitin-like proteins in autophagy. Biomed Res Int. 2014;Volume 2014. Article ID 832704. doi:10.1155/2014/832704

47. Tanida I, Miematsu-ikeguchi N, Ueno T, Kominami E. Lysosomal Turnover, but Not a Cellular Level, of Endogenous LC3 is a Marker for Autophagy. Autophagy. 2005;1: 84–91. doi:10.4161/cc.4.7.1796

48. Mizushima N, Yamamoto A, Hatano M, Kobayashi Y, Kabey Y, Suzuki K, Tokuhisa T, Yoshimori T. Dissection of autophagosome formation using Apg5-deficient mouse embryonic stem cells. J Cell Biol. 2001;152: 657–667. doi:10.1083/jcb.152.4.657

49. Hara T, Takamura A, Kishi C, Iemura S, Natsume T, Guan J L, Mizushima N. FIP200, a ULK-interacting protein, is required for autophagosome formation in mammalian cells. J Cell Biol. 2007;9: 497–510. doi:10.1083/jcb.200712064

50. Proikas-Cezanne T, Takacs Z, Dönnes P, Kohlbacher O. WIPI proteins: Essential PtdIns3P effectors at the nascent autophagosome. J Cell Sci. 2015;128: 207–217. doi:10.1242/jcs.146258

51. Noda T. Regulation of autophagy through TORC1 and mTORC1. Biomolecules. 2017;7: 1–10. doi:10.3390/biom7030052

52. Settembre C, Polito VA, Arencibia MG, Vetrini F, Erdin S, Erdin SU, Huynh T, Medina D, Colella P, Sardiello M, Rubinsztein DC, Ballabio A. TFEB Links Autophagy to Lysosomal Biogenesis. Science. 2011; 1429–1434.

53. Mizushima N. The role of the Atg1/ULK1 complex in autophagy regulation. Curr Opin Cell Biol. 2010;22: 132–139. doi:10.1016/j.ceb.2009.12.004

54. Fingar DC, Richardson CJ, Tee AR, Cheatham L, Tsou C, Blenis J. mTOR Controls Cell Cycle Progression through Its Cell Growth Effectors S6K1 and 4E-BP1/Eukaryotic Translation Initiation Factor 4E. Mol Cell Biol. 2004;24: 200–216. doi:10.1128/mcb.24.1.200-216.2004

55. Zatloukal B, Kufferath I, Thueringer A, Landegren U, Zatloukal K, Haybaeck J. Sensitivity and Specificity of *In situ* Proximity Ligation for Protein Interaction Analysis in a Model of

Steatohepatitis with Mallory-Denk Bodies. PLoS One. 2014;9. e96690

doi:10.1371/journal.pone.0096690

56. Hosokawa N, Hara T, Kaizuka T, Kishi T, Takamura A, Miura Y, Iemura S, Natsume T, Takehana K, Yamada N, Guan JL, Oshiro N, Mizushima N. Nutrient-dependent mTORC1 Association with the ULK1–Atg13–FIP200 Complex Required for Autophagy. Mol Biol Cell. 2009;20: 937–947. doi:10.1091/mbc.E08

57. Martina JA, Puertollano R. Rag GTPases mediate amino acid-dependent recruitment of TFEB and MITF to lysosomes. J Cell Biol. 2013;200: 475–491. doi:10.1083/jcb.201209135

58. Schalm SS, Blenis J. Identification of a conserved motif required for mTOR signaling. Curr Biol. 2002;12: 632–639. doi:10.1016/S0960-9822 (02)00762-5

59. Medina DL, Di Paola S, Peluso I, Armani A, De Stefani D, Venditti R, Montefusco S, Scotto-Rosato A, Prezopsp C, Forrester A, Settembre C, Wang W, Gao Q, Xu H, Sandri M, Rizzoto R, De Matteis MA, Ballabio A. Lysosomal calcium signalling regulates autophagy through calcineurin and TFEB. Nat Cell Biol. 2015;17: 288–299. doi:10.1038/ncb3114

60. McKeon F. When worlds collide: Immunosuppressants meet protein phosphatases. Cell. 1991;66: 823–826. doi:10.1016/0092-8674 (91)90426-Y

61. Aramburu J, Yaffe MB, López-Rodríguez C, Cantley LC, Hogan PG, Rao A. Affinity-driven peptide selection of an NFAT inhibitor more selective than cyclosporin A. Science. 1999;285: 2129–2133. doi:10.1126/science.285.5436.2129

62. Hagen BM, Boyman L, Kao JPY, Lederer WJ. A comparative assessment of fluo Ca^{2+} indicators in rat ventricular myocytes. Cell Calcium. 2012;52: 170–181. doi:10.1016/j.ceca.2012.05.010

63. Nakai J, Ohkura M, Imoto K. A high signal-to-noise Ca^{2+} probe composed of a single green fluorescent protein. Nat Biotechnol. 2001;19: 137–141. doi:10.1038/84397

64. Høyer-Hansen M, Bastholm L, Szyniarowski P, Campanella M, Szabadkai G, Farkas T, Bianchi K, Fehrenbancher N, Elling F, Rizzuto R, Mathiasen IS, Jaattela M. Control of Macroautophagy by Calcium, Calmodulin-Dependent Kinase Kinase-β, and Bcl-2. Mol Cell. 2007;25: 193–205. doi:10.1016/j.molcel.2006.12.009

65. Stewart AA, Ingebritsen TS, Manalan A, Klee CB, Cohen P. Discovery of A Ca^{2+}-and calmodulin-dependent protein phosphatase. FEBS Lett. 1982;137: 80–84. doi:10.1016/0014-5793(82)80319-0

66. Oka T, Sato K, Hori M, Ozaki H, Karaki H. Xestospongin C, a novel blocker of IP3 receptor, attenuates the increase in cytosolic calcium level and degranulation that is induced by antigen in RBL-2H3 mast cells. Br J Pharmacol. 2002;135: 1959–1966. doi:10.1038/sj.bjp.0704662

67. Yoshikawa, , T. Takahashi, S. Ichikawa, H. Takano, H. Tasaki, N. Yasuda M. Nito , Y. Tanigaki, T.and Kondo M. Effects of TJ-35 (Shigyakusan) on Gastric Mucosal Injury Induced by Ischemia-Reperfusion and Its Oxygen-Derived Free Radical-Scavenging Activities. J Clin Biochem Nutr. 1991;35: 189–196.

68. Ohta Y, Kobayashi T, Hayashi T, Inui K, Yoshino J. Preventive effect of Shigyaku-san on progression of acute gastric mucosal lesions induced by compound 48/80, a mast cell degranulator, in rats. Phyther reseatch. 2006;20: 256–262. doi:10.11339/jtm.23.101

69. Hashimoto D, Ohmuraya M, Hirota M, Yamamoto A, Suyama K, Ida S, Okumura Y, Takahashi E, Kido H, Araki K, Baba H, Mizushima N, Yamamura K. Involvement of autophagy in trypsinogen activation within the pancreatic acinar cells. J Cell Biol. 2008;181: 1065–1072. doi:10.1083/jcb.200712156

70. Chan EY. MTORC1 phosphorylates the ULK1-mAtg13-FIP200 autophagy regulatory complex. Sci Signal. 2009;2: 1–4. doi:10.1126/scisignal.284pe51

71. Pen S, Vega-rubin-de-celis S, Schwartz JC, Wolff NC, Tran TA, Zou L, Xie XJ, Corey DR, Brugarolas J. EMBO J. 2011;30: 3242–3258. doi:10.1038/emboj.2011.257

72. Decuypere JP, Bultynck G, Parys JB. A dual role for Ca^{2+} in autophagy regulation. Cell Calcium. 2011;50: 242–250. doi:10.1016/j.ceca.2011.04.001

73. Decuypere JP, Welkenhuyzen K, Luyten T, Ponsaerts R, Dewaele M, Molgó J, Agostinis P, Missiaen L, Parys JB, Bultynck G. Ins (1,4,5)P3 receptor-mediated Ca^{2+} signaling and autophagy induction are interrelated. Autophagy. 2011;7: 1472–1489. doi:10.4161/auto.7.12.17909

74. Kageyama S, Omori H, Saitoh T, Sone T, Guan JL, Akira S, Imamoto F, Noda T, Yoshimori T. The LC3 recruitment mechanism is separate from Atg9L1-dependent membrane formation in the autophagic response against Salmonella. Mol Biol Cell. 2011;22: 2290–2300. doi:10.1091/mbc.E10-11-0893

75. Hao F, Kondo K, Itoh T, Ikari S, Nada S, Okada M, Noda T. Rheb localized on the Golgi membrane activates lysosome- localized mTORC1 at the Golgi – lysosome contact site. J Cell Sci. 2018. doi:10.1242/jcs.208017

76. Saitoh T, Nakayama M, Nakano H, Yagita H, Yamamoto N, Yamaoka S. TWEAK induces NF-κB2 p100 processing and long lasting NF-κB activation. J Biol Chem. 2003;278: 36005–36012. doi:10.1074/jbc.M304266200

77. Chang C, Young LN, Morris KL, von Bülow S, Schöneberg J, Yamamoto-Imoto H, Oe Y, Yamamoto K, Nakamura S, Stjepanovic G, Hummer G, Yoshimori T, Hurley JH. Bidirectional Control of Autophagy by BECN1 BARA Domain Dynamics. Mol Cell. 2019;73: 339-353.e6. doi:10.1016/j.molcel.2018.10.035

78. Bloor S, Maelfait J, Krumbach R, Beyaert R, Randow F. Endoplasmic reticulum chaperone gp96 is essential for infection with vesicular stomatitis virus. Proc Natl Acad Sci U S A. 2010;107:6970-6975 doi:10.1073/pnas.0908536107

79. Sardiello M, Palimieri M, di Ronza A, Medina DL, Valenza M, Gennarino VA, Donaudy F, Polishchuk RS, Banfi S, Parenti G, Cattaneo E, Ballabio A. A Gene Network Regulating Lysosomal Biognesis and Function. Science. 2009;325: 473–477. doi:10.1126/science.1174447

Acknowledgements

I would like to express my heartfelt appreciation to Prof. Takeshi Noda, the world authority on autophagy and the person whom I respect from the bottom of my heart, for giving me such a wonderful opportunity to conduct this research, and for sometimes giving me such loving and strict guidance on my knowledge as a researcher. I am greatly appreciation Dr. Yasuhiro Araki, Dr. Shintaro Kira, Dr. Shiou-Ling Lu, Dr. Feike Hao, Dr. Kanae Noda, and Dr. Yo-hei Yamamoto for research guidance and discussion; All of lab members of Noda-Lab for discussion.

I would like to express my heartfelt gratitude to Prof. Takanobu Otomo for guidance and advice; Prof. Nobukazu Shitan and Dr. Yumi Nishiyama for cooperation in the field of herbal medicine.

I would like to thank Prof. Tamotsu Yoshimori and Dr. Maho Hamasaki for their knowledge, skills and support, guidance and advice on autophagy research in a wonderful environment to start this research; All of Yoshimori-Lab member for discussion.

I am grateful for the Tsumura Corporation (Tokyo, Japan) for the donation of Kampo medicines.

Finally, I would like to thank my friend Dr. Kenta Imai for giving me a chance to study, my parents for supporting me for my progress, and my daughter for always giving me the best smile and love.

Achievements

Publication

Sumiko Ikari, Shiou-Ling Lu, Feike Hao, Kenta Imai, Yasuhiro Araki, Yo-hei Yamamoto, Yumi Nishiyama, Chao-Yuan Tsai, Nobukazu Shitan, Tamotsu Yoshimori, Takanobu Otomo, Takeshi Noda. Starvation-induced autophagy via calcium-dependent TFEB dephosphorylation is suppressed by Shigyakusan. *PLOS ONE.* accept

Feike Hao, Kazuhiko Kondo, Takashi Itoh, Sumiko Ikari, Shigeyuki Nada, Masato Okada, Takeshi Noda. Rheb localized on the Golgi membrane activates lysosome-localized mTORC1 at the Golgi–lysosome contact site. *Journal of Cell Science.* 2018;131:jcs208017 doi:10.1242/jcs.208017

Meetings

碇純子, 今井健太, 濱崎万穂, 士反伸和, 吉森保.

オートファジーを制御する漢方薬の探索.

第９回オートファジー研究会 2015年11月15日～11月17日 兵庫県 淡路　淡路夢舞台国際会議場

碇純子, 呂 婷菱, 荒木保弘, Hao Feike, 今井健太, 士反伸和, 吉森保, 大友孝信, 野田健司.

漢方薬によるオートファジー活性制御機構

第65回年会日本生薬学会, 2018年9月15日～9月18日 広島県広島市　安田女子大学

碇純子, 呂 娉菱　荒木保弘, Hao Feike, 今井健太, 士反伸和, 吉森保, 大友孝信, 野田健司.

オートファジー活性を抑制する漢方薬の作用機序の解析

第91回日本生化学会大会 2018年9月24日～9月26日 京都府 国立京都国際会館

碇純子, 呂 娉菱, 荒木保弘, Hao Feike, 今井健太, 士反伸和, 吉森保, 大友孝信, 野田健司.

オートファジー活性を抑制する漢方薬の作用機構の解析

第11回オートファジー研究会 2018年11月21日　静岡県 つま恋リゾート彩の郷

碇純子, 呂 娉菱, 荒木保弘, Hao Feike, 今井健太, 士反伸和, 吉森保, 大友孝信, 野田健司.

オートファジー活性を抑制する漢方薬の作用機序の解析

第71回日本細胞生物学会 2019年6月24日～6月25日 兵庫県　神戸国際会議場

碇純子, 呂 娉菱, 荒木保弘, Hao Feike, 今井健太, 士反伸和, 吉森保, 大友孝信, 野田健司.

オートファジー阻害活性を有する漢方薬の作用機構の解析

第12回オートファジー研究会 2019年10月24日～10月27日　静岡県 つま恋リゾート彩の郷

Sumiko Ikari, Shiou Ling Lu, Yasuhiro Araki, Hao Feike, Kenta Imai, Nobukazu Shitan, Tamotsu Yoshimori, Takanobu Otomo, Takeshi Noda.

Mechanisms of Action of Japanese traditional medicine on Autophagy

The 9th International Symposium on Autophagy 2019年11月3日～11月7日 Taipei, Taiwan